



Contents lists available at ScienceDirect

Science of the Total Environment

journal homepage: www.elsevier.com/locate/scitotenv

Meta-analysis of uranium contamination in groundwater of the alluvial plains of Punjab, northwest India: Status, health risk, and hydrogeochemical processes

Prafulla Kumar Sahoo ^{a,b,*}, Hardev Singh Virk ^c, Mike A. Powell ^d, Ravishankar Kumar ^a, Jitendra Kumar Pattanaik ^e, Gabriel Negreiros Salomão ^b, Sunil Mittal ^a, Lokesh Chouhan ^a, Yugalakshmi Kadapakkam Nandabalan ^a, Raghavendra Prasad Tiwari ^a

^a Department of Environmental Science and Technology, Central University of Punjab, V.P.O. Ghudda, 151401 Bathinda, India

^b Instituto Tecnológico Vale (ITV), Rua Boaventura da Silva, 955, Belém 66055-090, PA, Brazil

^c SGGS World University, Fatehgarh Sahib 140407, Punjab, India

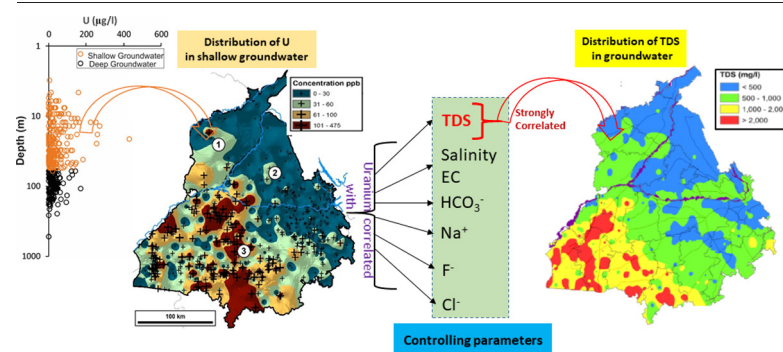
^d Department of Renewable Resources, University of Alberta, Edmonton, AB T6G 2R3, Canada

^e Department of Geology, Central University of Punjab, V.P.O. Ghudda, Bathinda 151401, India

HIGHLIGHTS

- Uranium contamination is very severe in shallow aquifers (<60 m) of South-west Punjab, India.
- High TDS and saline condition act as the major controlling factors for U enrichment.
- Samples with TDS >1000 mg l⁻¹, ORP >300 mV & pH >7 have a greater chance of U > 30 ppb.
- U-F co-occurrence is pronounced in shallow aquifers of South-west Punjab.
- U is mainly geogenic origin, but arid climatic & agrochemical factors increase U mobilization.

GRAPHICAL ABSTRACT



ARTICLE INFO

Article history:

Received 15 June 2021

Received in revised form 7 November 2021

Accepted 13 November 2021

Available online xxxx

Editor: Manish Kumar

Keywords:

Uranium enrichment

Shallow aquifer

Salinity

Geogenic contamination

Agrochemicals

Punjab

ABSTRACT

Despite numerous studies, there are many knowledge gaps in our understanding of uranium (U) contamination in the alluvial aquifers of Punjab, India. In this study, a large hydrogeochemical dataset was compiled to better understand the major factors controlling the mobility and enrichment of uranium (U) in this groundwater system. The results showed that shallow groundwaters (<60 m) are more contaminated with U than from deeper depths (>60 m). This effect was predominant in the Southwest districts of the Malwa, facing significant risk due to chemical toxicity of U. Groundwaters are mostly oxidizing and alkaline (median pH: 7.25 to 7.33) in nature. Spearman correlation analysis showed that U concentrations are more closely related to total dissolved solids (TDS), salinity, Na, K, HCO_3^- , NO_3^- , Cl^- , and F^- in shallow water than deep water, but TDS and salinity remained highly correlated (U-TDS: $\rho = 0.5$ to 0.6; U-salinity: $\rho = 0.5$). This correlation suggests that the salt effect due to high competition between ions is the principal cause of U mobilization. This effect is evident when the U level increased with increasing mixed water species (Na-Cl, Mg-Cl, and Na-HCO₃). Speciation data showed that the most dominant U species are $\text{Ca}_2\text{UO}_2(\text{CO}_3)^{2-}$ and $\text{CaUO}_2(\text{CO}_3)^{3-}$, which are responsible for the U mobility. Based on the field parameters, TDS along with pH and oxidation-reduction potential (ORP) were better fitted to U concentration above the WHO guideline value (30 $\mu\text{g L}^{-1}$), thus this combination could be used as a quick indicator of U contamination. The strong positive correlation of U with

* Corresponding author at: Department of Environmental Science and Technology, Central University of Punjab, V.P.O. Ghudda, 151401 Bathinda, India.

E-mail address: prafulla.iitkgp@gmail.com (P.K. Sahoo).

F^- ($\rho = 0.5$) in shallow waters indicates that their primary source is geogenic, while anthropogenic factors such as canal irrigation, groundwater table decline, and use of agrochemicals (mainly nitrate fertilizers) as well as climate-related factors i.e., high evaporation under arid/semi-arid climatic conditions, which result in higher redox and TDS/salinity levels, may greatly affect enrichment of U. The geochemical rationale of this study will provide Science-based-policy implications for U health risk assessment in this region and further extrapolate these findings to other arid/semi-arid areas worldwide.

1. Introduction

Groundwater is a major resource for drinking, agriculture, and industrial uses worldwide (Mukherjee et al., 2020). Particularly in India, more than 80% of drinking water supplies and 89% of irrigated agriculture are met by groundwater (CGWB, 2019; Mukherjee et al., 2020). However, in the recent years, this resource has been under great threat both in terms of quantity and quality (Jumulana et al., 2020; Kumar et al., 2020a; Mukherjee et al., 2020). In groundwater quality, geogenic contamination is mainly caused by As and F and their co-occurrence has long been recognized as most the widespread threat across the globe (Alarcón-Herrera et al., 2013; Alcaine et al., 2020; Bhattacharya et al., 2006; Kumar et al., 2020a; Scanlon et al., 2009). This is in fact the case in India, especially in alluvial plains of the major river basins like the Indo-Gangetic and Brahmaputra basins (Das et al., 2017; Das et al., 2018; Kumar et al., 2016; Mukherjee et al., 2012; Mukherjee et al., 2015; Patel et al., 2019a; Patel et al., 2019b). Recently, uranium (U) occurrence has emerged as an issue of national importance in India as it is found in high concentrations ($>30 \mu\text{g/L}$; World Health Organization (WHO, 2017) provisional guideline value for U concentration in drinking water) in more than 16 states (Coyte et al., 2018). These high concentrations of U are directly linked with serious health hazards (CGWB, 2020; Virk, 2017a; Virk, 2017b). This a predominant problem in the Northwestern states which are associated with alluvial aquifers, and also up to some extend in the southern and southeastern aquifers, which are primarily associated with crystalline basement rocks (CGWB, 2020; Coyte et al., 2018). U toxicity comes from its both chemical and radiological properties, but the former is of greater concern (Rump et al., 2019). Elevated levels of U in water lead to chronic kidney, liver, and lung damage while long-term exposure to U through drinking water is associated with nephrotoxic effects (Bangotra et al., 2021; Zamora et al., 1998).

U is a naturally occurring radioactive element commonly present in rocks and soils in various forms like uraninite (UO_2), coffinite (USiO_4), pitchblende (U_3O_8), autunite ($\text{Ca}(\text{UO}_2)_2(\text{PO}_4)_2 \cdot 10\text{-}12\text{H}_2\text{O}$), uranophane ($(\text{Ca}(\text{UO}_2)_2\text{SiO}_3(\text{OH})_2 \cdot 5\text{H}_2\text{O}$), etc. (Guthrie and Kleeman, 1986; Thivya et al., 2016; Smedley et al., 2006; Wu et al., 2014). Elevated U levels in groundwater are mainly associated with U mineralized zones or high-uranium bearing source rocks (like granites) (Coyte et al., 2018; Smedley et al., 2006; Wu et al., 2014). Uranium contamination can also occur from some of the main anthropogenic activities like mining and processing of uranium ore, nuclear waste disposal, and phosphate fertilizers (Conceicao and Bonotto, 2000; Sharma and Rishi, 2016). In groundwater, the solubility and mobility of U are highly dependent on factors like water-rock interactions, climatic conditions, and hydrogeochemical conditions including pH, redox potential, speciation, ionic strength, and the occurrence of bicarbonate and salinity (Chandrasekar et al., 2021; Langmuir, 1978; Maher et al., 2013; O'Loughlin et al., 2011; Wu et al., 2018). Under oxic/suboxic and alkaline pH ($\text{pH} > 7$) conditions, U is primarily present as hexavalent U(VI) in the form of uranyl ion (UO_2^{2+}) and it is associated with hydroxide and carbonate complexes, which are readily mobilized and highly soluble. On the contrary in reducing waters, U occurs as U(IV) which has a strong tendency to precipitate and to remain immobile (Kumar et al., 2011a). U(VI) readily interacts with other ions (e.g. OH^- , CO_3^{2-} , PO_4^{3-} , NO_3^- , SiO_4^{4-} , SO_4^{2-}) to form a range of soluble anionic complexes that enhance solubility and mobility (Cumberland et al., 2016; Thivya et al., 2016; Li et al., 2016). The mobility of U is also controlled by the presence of Fe-oxyhydroxides, clays and organic matter, which act as sinks (Wu et al., 2014). Anthropogenic factors such as excessive withdrawal of groundwater (which induced oxic

condition) and nitrate/phosphate pollution from mineral fertilizers can also be important for U mobilization (Coyte et al., 2018). Moreover, U behavior in groundwater can change significantly in an aquifer along the path from recharge to discharge processes (Thivya et al., 2016). These studies highlight that U dynamics in alluvial aquifers are complex, and impacted by both natural and anthropogenic sources; this is true for the Indo-Gangetic basin, especially the Punjab basin (India), where agricultural activity is predominant.

Punjab is the worst U affected State in India (CGWB, 2014; Pant et al., 2017; Coyte et al., 2018; Virk, 2017a; Virk, 2017b; Virk, 2019a; Virk, 2019b). Uranium contamination rates have soared recently in the Malwa region, South-western Punjab, which is known as the “cancer belt” or “cancer capital” of India (Virk, 2017a; Virk, 2017b). This is evidenced in several previous studies (Table S1) which have reported U concentrations in groundwater in community water systems and in private wells of Punjab. Overall, these studies show that shallow groundwaters have higher concentrations of U, which is due to higher redox potential (oxic conditions) and higher HCO_3^- concentrations. Several hypotheses have been emerged which attribute the origin of these high groundwater U levels in this region such as excess application of phosphate fertilizers, coal fly ash from thermal power stations, the gulf war, and the geology of the Tosham Hill granite or sediments derived from the Himalayas (Alrakabi et al., 2011; Patnaik et al., 2016). However, the existing explanations on the source and processes responsible for U contamination are still inconclusive, and require further work. Furthermore, considering the increasing salinity level in the shallow aquifers of Punjab (Krishan et al., 2021), it is necessary to evaluate the risk of salinization on U mobilization in the region. In addition, developing U baseline levels for the State is crucial for future studies and to inform policy related to acceptable groundwater resources and use.

Taking into account the above factors, the present study evaluated a large body of hydrochemical groundwater data (obtained from published literature and the government website) to provide a comprehensive view of the occurrence and distribution of groundwater U in the Punjab State. This research has been designed through the following hypotheses: 1) U contamination is significantly different between shallow and deep aquifers; 2) U contamination is severe in the southwest of Malwa region; 3) groundwater salinity/total dissolved solids (TDS) driven by climate and agrochemical factors play a major role in U mobilization in the region; and 4) a preliminary indicator of U contamination can be established based on field-based parameters. The findings of this work are intended to inform policy related to U risk assessment, plan future drinking water projects, attenuate the U intake from current drinking water projects, and predict changes in U behavior and distribution in existing aquifers based on climate change and agrochemical factors within Punjab State. Finally, an extrapolation of the findings to other parts of India and worldwide will be persuaded.

2. Study area

The Punjab State (between latitudes $29^\circ 32'$ and $32^\circ 28'N$ and longitudes $73^\circ 50'$ and $77^\circ 00'E$) is located in the North-western part of India (Fig. 1a). It occupies a geographic area of $50,362 \text{ km}^2$ at an average elevation of 200 m above mean sea level. The state is subdivided into three major regions: Malwa (comprising 65.1%, with 11 districts); the other two are Majha and Doaba and are predominantly agrarian with 85% of the geographic area under cultivation as compared to the national average of 40.38% (Krishan et al., 2021). The land use and land cover map (Fig. 1a) shows that cropland dominates (86.23%), while some forest cover

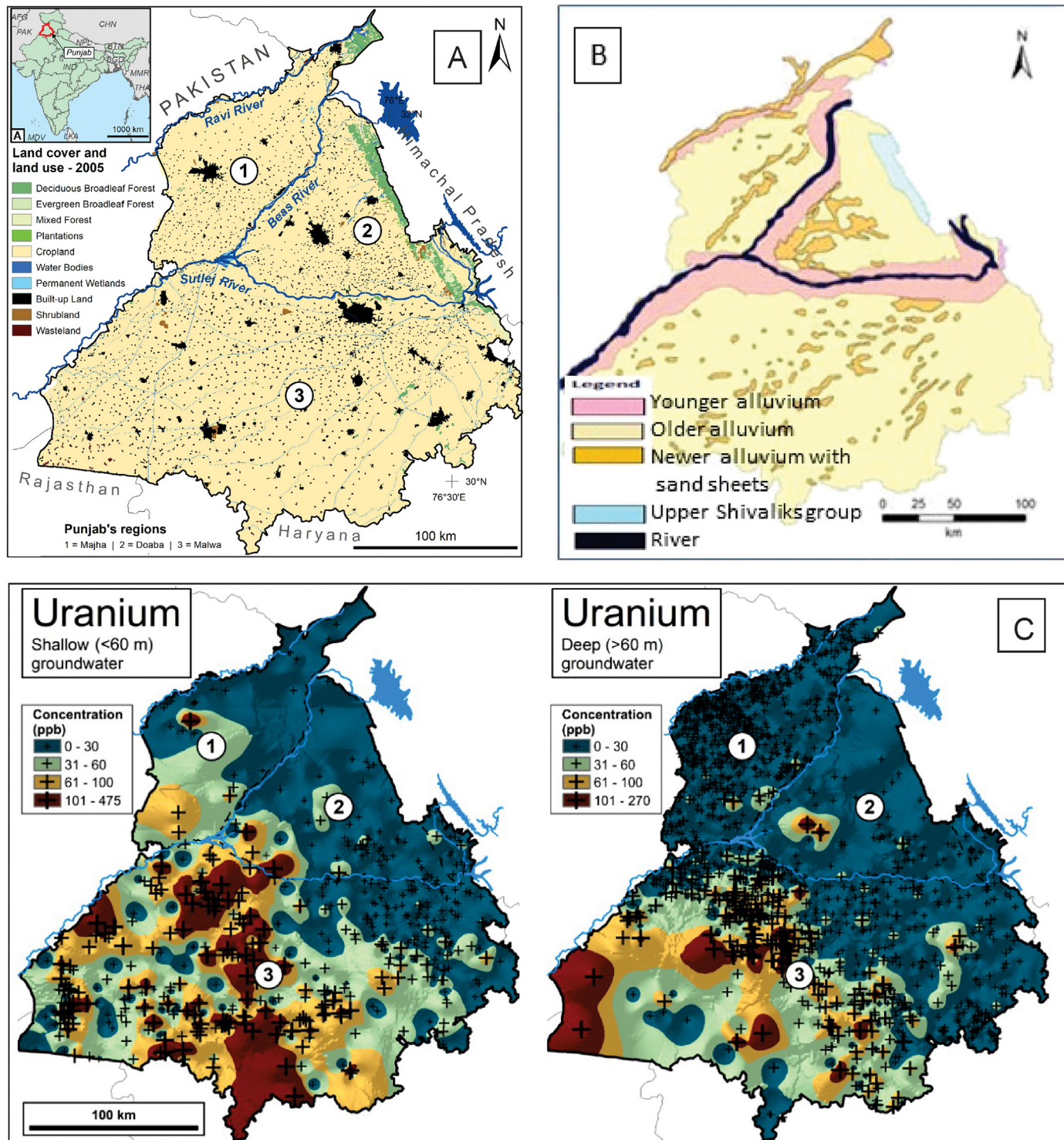


Fig. 1. (a) Location map of the Punjab state in India and the land-use and land cover pattern within the state based on 2005 (Roy et al., 2016), (b) general geology of the state (GSI, 2011), and (c) spatial distribution of uranium concentration ($\mu\text{g l}^{-1}$) in shallow (<60 m) and deep (>60 m) groundwaters of Punjab, India.

(3.03%) exists in the northeastern region (Roy et al., 2016). Paddy and cotton are the main Kharif crops while wheat is the main rabi crop grown in the region. Punjab lies in the Indus basin and is drained by three major perennial rivers: the Sutlej, Beas, and Ravi (Fig. 1a) (CGWB, 2021). All rivers flow in a southwest direction except the Satluj River which flows in the southwestern part of the State, mainly flows from east to west up towards Harike and from Harike it flows south-westerly towards Fazilka.

2.1. Geology of the basin

Punjab sits on a flat alluvial plain, part of the Indo-Gangetic alluvial plain, and it is formed by the deposition of sediments derived from the Himalayan mountains. Its thickness varies laterally and steadily decreases southwardly where the basement lies at shallow depths (CGWB, 2014; CGWB, 2021). The alluvium is heterogeneous, ranges in age from Upper Pleistocene to Recent, and is generally classified as Older and Younger (Fig. 1b; GSI, 2011). The Older alluvium was deposited mainly by rivers

originating from the Himalayas during the Middle to Upper Pleistocene age and is composed of sand and loam with kankar, sticky clay, grey medium to coarse micaceous sand with kankar surrounded to sub angular unsorted pebbles, gravel and cobbles from adjacent foothills (CGWB, 2014; CGWB, 2021). The Younger alluvium was deposited from Upper Pleistocene to Recent age, and is comprised of coarse- to medium-grained sand with lesser amounts of silt and clay, undifferentiated aeolian flat/ sand sheets, blue-grey to light micaceous sand with inter-bands of purple-red clay, undifferentiated semi-consolidated and stabilized older dunes with kankar and some carbonaceous materials (CGWB, 2014). The soil of the Punjab region is largely developed on fluvial alluvium (CGWB, 2021). They are mostly loose, sandy textured, and calcareous with an admixture of gravel, sand, silt, and clay in varying proportions. Kankar, which is an impure calcium carbonate in the form of irregular nodules and concretions, is frequently observed at depths of 60–200 cm below the surface or even at the surface of some agricultural fields.

2.2. Groundwater system

The groundwater in the region occurs in both unconfined shallow aquifer and semi-confined/confined deeper aquifers; both aquifers are recharged by canal irrigation and rainfall (CGWB, 2014; CGWB, 2021; Krishan et al., 2021). The vertically extensive and persistent aquifers in the State occur in granular zones of fine to medium sand with clay intercalations. However, towards the southwestern areas the thickness of freshwater aquifers is much thinner compared to the other areas and is underlain by brackish/saline water (CGWB, 2021). In the southwestern part, the thickness of freshwater sediments varies from 10 to 200 m, decreasing towards the extreme southwestern edge of the State where it is less than 10 m, while in the northeastern part of the State the thickness of freshwater sediments is greater than 450 m (Gupta, 2011). These characteristics define two distinct topographical and hydro-geological settings within Punjab, i.e., high-yielding fresh groundwater regions in northern and central districts and the saline groundwater regions in southwestern districts. Major groundwater recharge areas occur in the mountains and hills in northern and northeastern Punjab, which are more elevated than the southwest areas, thus resulting in an overall groundwater flow from the northeast to the southwest with a rise of water levels (Fig. S1a). Water-logging and increased soil salinity (due to evaporation of canal water) in low-lying districts to the southwest, mainly in Bathinda, Muktsar, Fazilka, and Ferozepur (Fig. S1a) (which rely heavily on canal irrigation) are also due to continuous seepage of water from unlined canals and distributaries (Krishan et al., 2021). Also, the water level has highly fluctuated in this region, being highly declined water level in the southwest region compared to the northeast (Fig. S1b). The Central Groundwater Board (CGWB) uses a convention of dividing groundwater into <60 m bgl and >60 m bgl, based on typical well depths from different types of well production; this convention is used here in order to maintain consistency with CGWB reporting.

2.3. Climate

Punjab climate is semi-humid to semi-arid in the north, arid in the south and southwest, and semi-arid in the remaining part of the State. The State experiences cold winters from early December to the end of February and hot summers from mid-April to the end of June with temperatures ranging from 5 °C to 50 °C. The rainy season ranges from early July to the end of September which contributes around 80% of the annual rainfall (i.e., 600 mm) (Krishan et al., 2021). The Siwalik hills region close to the Himalayan range receives maximum rainfall of >1000 mm yr⁻¹ while part of the eastern region receives rainfall >750 mm yr⁻¹. The extreme southwest region of the State receives much lower rainfall compared to the north and southeast. The southwest monsoon contributes about 80% of the rainfall responsible for groundwater recharge.

3. Materials and methods

3.1. Data collection and analytical methods

The data used in this study were obtained from published literatures at the Central University of Punjab (CUP; Jaswal et al., 2021; Kumar et al., 2020b; Kumar et al., 2021; Mittal et al., 2021), British Geological Survey (BGS; Lapworth et al., 2017), and from the Department of Water Supply and Sanitation, Punjab State, Mohali database (DWSS; Ministry of Water Resources, Government of India). The compiled database was screened to include only those samples monitored within the last 12 years, and containing U concentrations and/or other water quality parameters along with depth information. This is further selected based on the U analysis method by Inductively Coupled Plasma Mass Spectrometry (ICP-MS) and with a charge-balance error within 15%. This produced approximately 2050 groundwater records from all Punjab Districts which were collected from 2016 to 2017 for CUP, 2013–2014 for BGS, and 2010 to 2016 for DWSS (Table S2). Of the entire dataset, about 480 samples from 12 districts (mostly CUP and BGS data), contained both U and other chemical and physico-chemical parameters like pH, dissolved oxygen (DO), oxidation-reduction potential (ORP), salinity, electrolytic conductivity (EC), total dissolved solid (TDS), Ca²⁺, Mg²⁺, Na⁺, K⁺, Fe, Cl⁻, NO₃⁻, SO₄²⁻, and HCO₃⁻, which were considered for this meta-analysis, while DWSS data complemented only the U distribution and health risk plots. In each of the references used here, sample collection, handling and process varied, but most followed standard protocols. For more detailed information regarding the data compilation, sampling techniques, analytical methods and quality control data, see Supplementary Note 1.

3.2. Statistical analysis and spatial maps

Descriptive statistics were used to characterize the dataset (minimum, maximum, mean, median, standard deviation, coefficient of variation (CV), and quantiles (Q1, Q3)). The assumption of normality for water quality variables was checked using numerical techniques (e.g., Shapiro-Wilk and Kolmogorov-Smirnov test). Since most of the variables do not follow a normal distribution (Table S3), Spearman's rank correlation coefficient (ρ values) was used to identify the relationship between parameter pairs. Multivariate statistical analyses including Principal Component Analysis (PCA) and Hierarchical Cluster Analysis (HCA) were carried out on log-transformed data to identify the important clusters or relations between different hydrogeochemical parameters. Principal components (PCs) with Eigenvalues >1 were selected for this study. Ward's method with squared Euclidian distance was used for HCA after Z score standardization to validate the PCA results by recognizing identical clusters or groups of hydrogeochemical variables based on similarities and pairing in successive steps (Das et al., 2018). A non-parametric ANOVA (Kruskal Wallis test) was performed on all water quality data to test significant differences of mean values for the chemical elements between shallow and deep groundwaters. The null hypothesis for this test is that the mean elemental concentrations of water between shallow and deep groundwater are not significantly different at $p > 0.05$. All statistical analyses were performed using the software SPSS (Statistical Package for the Social Sciences, version 18) and Minitab (version 11). Spatial distribution maps of U and its health risk index were carried out using the spatial interpolation method by Inverse Distance by the Geographic Information System (GIS) (ArcGIS 10.6) under the World Geodetic System 1984 (WGS84) datum. The non-carcinogenic health risk (Hazard Quotient: HQ) of U was estimated using the standard methodology of USEPA (US Environmental Protection Agency, 1989, 2001); for details of calculation see Supplementary Note 2.

3.3. Speciation and saturation index calculation

U speciation modeling and saturation index (SI) of various secondary mineral phases of groundwater samples were calculated using the GSS module of the Geochemist's Workbench® (Student Version, Edition 12)

and the commonly employed thermodynamic database “thermo.tdat”. Saturation Index (SI) was calculated based on the equation: $SI = \log(IAP/K_{SP})$ (Deutsch, 1997). ‘IAP’ denotes the Ion Activity Product, and ‘ K_{SP} ’ is the solubility product constant, which is the equilibrium constant for the dissolution of a solid in water. If $IAP < K_{SP}$, $SI < 0$, the solution is undersaturated and the minerals are likely to dissolve; and if $IAP > K_{SP}$, $SI > 0$, the solution is supersaturated and minerals are likely to precipitate. The speciation of uranium was calculated by the SpecE8 program using the Debye-Hückel method.

4. Results and discussion

4.1. Basic hydrochemical characteristics between shallow and deep groundwater

The descriptive statistics of the chemical parameters in both shallow and deep groundwater samples are presented in Table 1. Results show considerable variation between mean and median values for several parameters, which have larger standard deviations (SD). In most cases, the SD for shallow groundwater parameters is larger compared to deep waters. This is consistent with the coefficient of variation (CV%), which reflects a higher degree of variability (>100%) in the case of U, Cl^- , NO_3^- , SO_4^{2-} , Na^+ , K^+ , and Fe in both water types, but highest for shallow groundwaters. It is likely that multiple factors are contributing to this variability. This can be further

seen in the Kruskal Wallis test results (Table S4), which show that there is a statistically significant difference (p -value <0.05) between shallow and deep samples for a range of parameters, except pH, and Fe. This can also be seen from their vertical distributions (Fig. 2). The pH ranged from 6.02 to 8.5 with median pH 7.25 and 7.33 in shallow and deep groundwater respectively (Table 1), indicating the mostly alkaline nature of groundwater. This is due to the dominance of carbonate minerals in sediments. Shallow groundwaters are more saline (median salinity 368 mg l^{-1}) than deep waters (median salinity 312 mg l^{-1}). Similarly, very high EC and TDS in the shallow water ($223\text{--}4740 \mu\text{S}$ and $164\text{--}3175 \text{ mg l}^{-1}$, respectively) compared to deep water ($41\text{--}2300 \mu\text{S cm}^{-1}$ and $29\text{--}1430 \text{ mg l}^{-1}$, respectively) (Table 1) are due to more weathering and dissolution of salts along with anthropogenic input with rapid recharge of water through shallow aquifers. As per the groundwater classification of Freeze and Cherry (Freeze and Cherry, 1979), deep groundwaters are mostly classified as freshwater ($\text{TDS} < 1000 \text{ mg l}^{-1}$), while a significant number of shallower waters are classified as brackish ($\text{TDS} < 1000\text{--}10,000 \text{ mg l}^{-1}$). ORP varies from 109 to 485 mV (median 370 mV) to 221 mV to 460 mV (median 382 mV) in shallow and deep groundwater, respectively (Table 1), indicating the dominance of oxic conditions in both aquifers; this agrees with the DO analyses, even though some samples (<10%) were sub-oxic and more reducing at depths. The shallow groundwaters are dominated by cations, Ca^{2+} , Mg^{2+} , and Na^+ and anions, HCO_3^- , Cl^- , SO_4^{2-} , and NO_3^- , while

Table 1

Descriptive statistics for uranium (U) and other physicochemical parameters in shallow (<60 m) and deep (>60 m) groundwater of Punjab. This synthesis is based on data from 12 districts, except U, which accounts all districts (for details, see Supplementary Note 1).

Variable	Unit	N	Min	Med	Mean	StDev	Q1	Q3	Max	CV(%)
Shallow groundwater										
Depth	meter	279	3.04	30.48	28.614	14.79	15.24	39.63	60	52
U	$\mu\text{g l}^{-1}$	554	0.15	28.16	50.9	67.01	7.7	66	476.5	131
pH		279	6.41	7.25	7.28	0.36	7.01	7.5	8.5	5
EC	$\mu\text{S/cm}$	279	223	845	1053.2	688.4	603	1382	4740	65
TDS	mg l^{-1}	258	164	580.5	728.7	465.1	423.9	928.3	3175	64
ORP	mV	258	109	370.5	348.0	276.9	249.3	409	485	52
Salinity	mg l^{-1}	193	0	368	433.4	282.3	278	510.5	1973.7	65
DO	mg l^{-1}	261	0.175	3.42	3.33	1.12	2.56	4.12	6.55	34
F ⁻	mg l^{-1}	279	0.09	0.80	1.34	1.24	0.51	1.96	8.23	93
Cl ⁻	mg l^{-1}	279	5.64	52.48	98.51	111.69	32.49	131.16	832.45	113
NO ₃ ⁻	mg l^{-1}	279	0.02	15.9	29.7	39.59	4.55	37.59	221.33	133
SO ₄ ²⁻	mg l^{-1}	279	0	41.15	85.72	119.66	19.91	112.82	967.34	140
PO ₄ ³⁻	mg l^{-1}	258	0.09	0.1	0.16	0.102	0.1	0.18	0.72	65
HCO ₃ ⁻	mg l^{-1}	279	84	400.0	399.15	162.83	265	515	1025	41
Na	mg l^{-1}	279	1.71	66.55	100.14	101.48	32.42	140.4	688.5	101
K	mg l^{-1}	278	0	6.805	9.12	10.96	3.792	10.03	97.04	120
Ca	mg l^{-1}	275	2.52	90	92.59	62.68	38.55	130	370	68
Mg	mg l^{-1}	275	5.54	150	182.44	139.55	70	284	900	76
Fe	$\mu\text{g l}^{-1}$	214	3.7	240.2	580.10	675.80	107.1	964.7	3508.5	116
Deep groundwater										
Depth	meter	209	60.96	91.46	106.25	54.61	76.21	121.95	518.29	51
U	$\mu\text{g l}^{-1}$	1508	0.02	10.1	22.2	33.2	2.7	25	275	143
pH		209	6.02	7.33	7.36	0.33	7.14	7.57	8.38	5
EC	$\mu\text{S/cm}$	209	41	604	670.8	287.4	499.5	798	2300	43
TDS	mg l^{-1}	192	29	431.9	474.9	194.1	357.8	561.3	1430	41
ORP	mV	192	221	396	382.54	240.15	266.25	409	460	22
Salinity	mg l^{-1}	188	22	312	345.5	141.4	261.3	413.5	1173	41
DO	mg l^{-1}	195	0.11	3.65	3.60	0.90	3.08	4.2	5.8	25
F ⁻	mg l^{-1}	209	0.05	0.7	0.90	0.638	0.53	1.027	3.91	70
Cl ⁻	mg l^{-1}	209	1.61	29.99	34.00	44.73	14.99	47.48	307.38	109
NO ₃ ⁻	mg l^{-1}	209	0.02	12.05	19.47	27.28	2.44	24.89	198.65	140
SO ₄ ²⁻	mg l^{-1}	209	1	21.33	34.5	40.33	9.53	45.03	276.81	117
PO ₄ ³⁻	mg l^{-1}	192	0.1	0.111	0.171	0.11	0.1	0.2	0.83	65
HCO ₃ ⁻	mg l^{-1}	209	60	415	409.56	116.22	350	485	805	28
Na	mg l^{-1}	209	1	47.08	70.13	61.29	31.59	87.05	315.65	87
K	mg l^{-1}	209	0	5.06	6.487	8.476	2.775	7.63	89.11	131
Ca	mg l^{-1}	207	5	91	93.22	46.63	60	125	300	50
Mg	mg l^{-1}	207	5.5	215	201.53	111.8	120	271	620	55
Fe	$\mu\text{g l}^{-1}$	204	3.5	320.6	571	762.8	133.6	734.3	6946.9	134
Depth	meter	209	60.96	91.46	106.25	54.61	76.21	121.95	518.29	51

N: number of samples; Min: minimum; Max: maximum; StDev: standard deviation; CV: coefficient of variation; Q1 and Q2: lower (first) and upper (third) quartile, respectively. TDS: total dissolved solids; ORP: oxidation-reduction potential; EC: electrolytic conductivity.

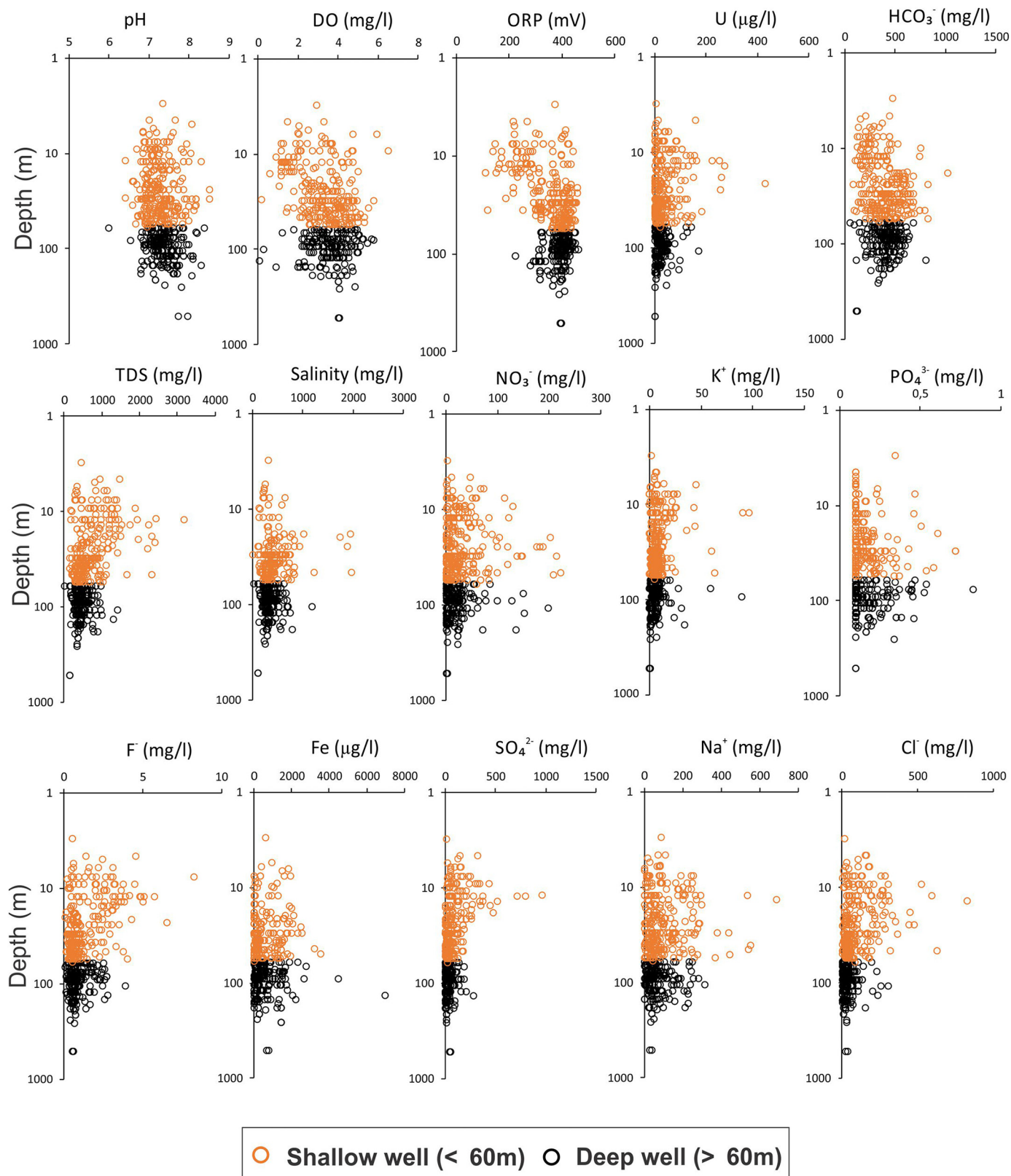


Fig. 2. Variation of water quality parameters (pH, DO, ORP, U, HCO_3^- , TDS, salinity, NO_3^- , K^+ , PO_4^{3-} , F^- , Fe, SO_4^{2-} , Na^+ and Cl^-) between shallow (<60 m) and deep (>60 m) groundwaters of Punjab, India.

the deeper waters are dominated by Ca^{2+} , Mg^{2+} , Na^+ and HCO_3^- . Based on median concentrations, the major anions followed the trend, $\text{HCO}_3^- > \text{Cl}^- > \text{SO}_4^{2-} > \text{NO}_3^- > \text{F}^-$ in both waters, but the levels of Cl^- , SO_4^{2-} , NO_3^- and F^- were mostly higher in shallow groundwater and some

exceeded their respective World Health Organization (WHO, 2017) drinking water permissible limits of $\text{NO}_3^- (50 \text{ mg l}^{-1})$, $\text{SO}_4^{2-} (250 \text{ mg l}^{-1})$, $\text{Cl}^- (200 \text{ mg l}^{-1})$ and $\text{F}^- (1.5 \text{ mg l}^{-1})$. Based on the median concentrations, the occurrence of cations followed the order $\text{Mg}^{2+} > \text{Ca}^{2+} > \text{Na}^+ > \text{K}^+$.

The median values of Mg^{2+} were slightly higher in deeper water than shallow water (215 and 150 mg l⁻¹, respectively); Ca^{2+} median values remained similar in both waters (91 mg l⁻¹ vs 90 mg l⁻¹, respectively) and Na^+ was more abundant in shallower groundwater. Overall, it is worth noting that major ion concentrations are higher at shallow depth than the deeper aquifer groundwater (Table 1; Fig. 2).

4.2. Groundwater evolution and weathering

Piper trilinear plots (Piper, 1944; Fig. 3a, b) and bivariate plots (Fig. 4a–e) were used to understand the sources of major ions and the complex hydrochemical processes that control groundwater chemistry (Chandrasekar et al., 2021; Kumar et al., 2009). As shown in Fig. 3a, most of the deep waters

(about 75%) are classified as Mg-HCO₃ type, with <25% of the samples being mixtures of alkali and alkaline earth types, and dominance of weakly acidic anions over strongly acidic anions (i.e., HCO₃⁻ > Cl⁻ or SO₄²⁻). The dominance of Mg-HCO₃ species associated with low salinity in deep groundwater suggests rock weathering as the predominant process for controlling groundwater chemistry. However, in shallow groundwater, where salinity is high, the dominant Mg-HCO₃ species decreases with increasing mixed facies such as Na-HCO₃, Na-Cl, and Mg-Cl types; a similar observation was made by Chandrasekar et al. (2021). This is due to the greater mixing of surface and groundwater, more agrochemical inputs from surface waters, and the role of evaporation. The mixing process can lead to the desorption and/or dissolution of more secondary minerals (including salts) in the shallow aquifers.

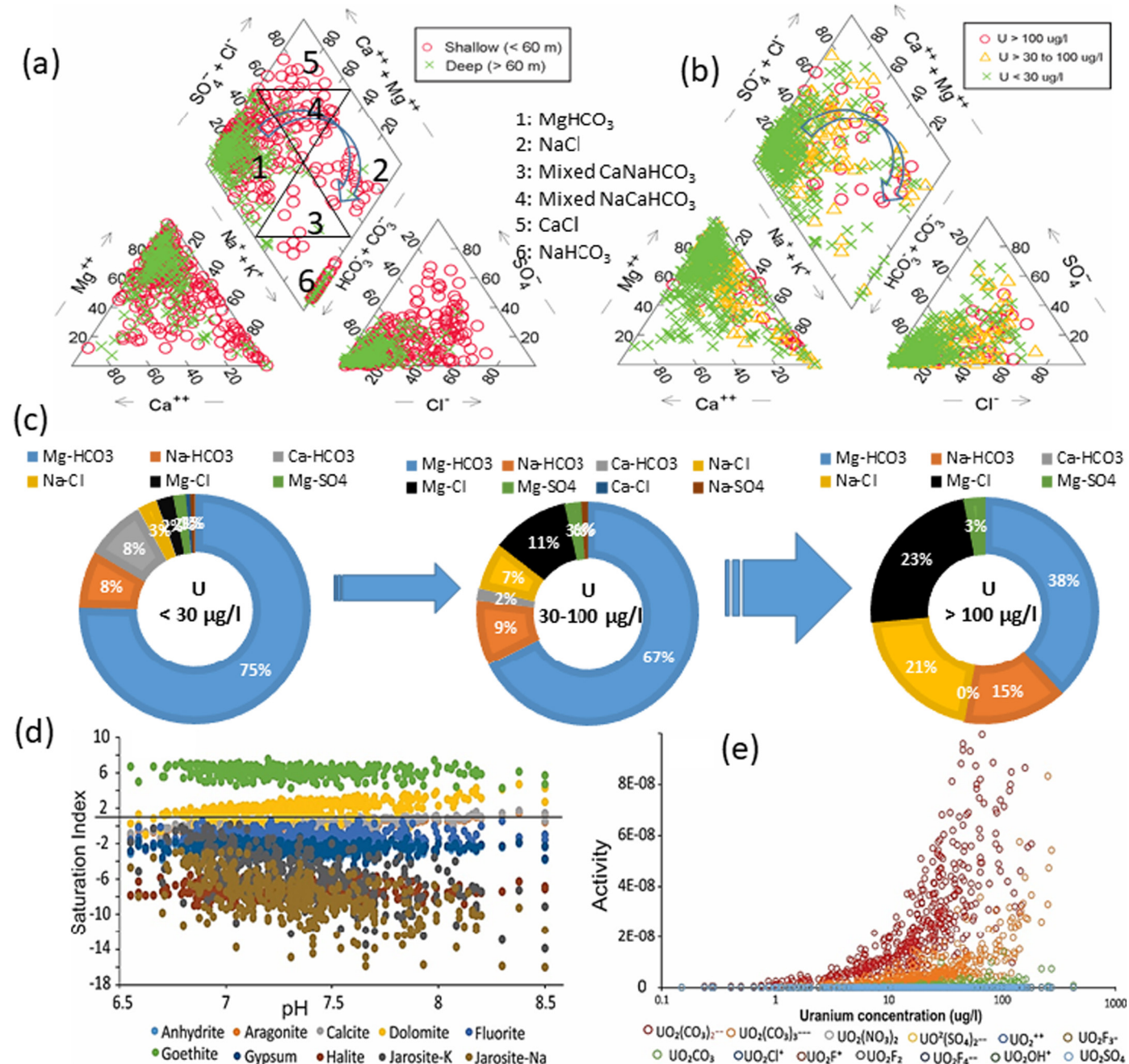


Fig. 3. Piper plot depicting major hydrogeochemical facies/water types from (a) shallow vs. deep groundwaters and (b) their influence on U concentrations; (c) percentage of water facies with respect to different U concentrations which shows that Mg-HCO₃ species dominate all three U categories, and decrease as the U concentration increases with increasing of Na-Cl, Mg-Cl and Na-HCO₃ facies; and (d) saturation indices of various secondary mineral phases and (e) uranium species in the groundwater samples of Punjab, India.

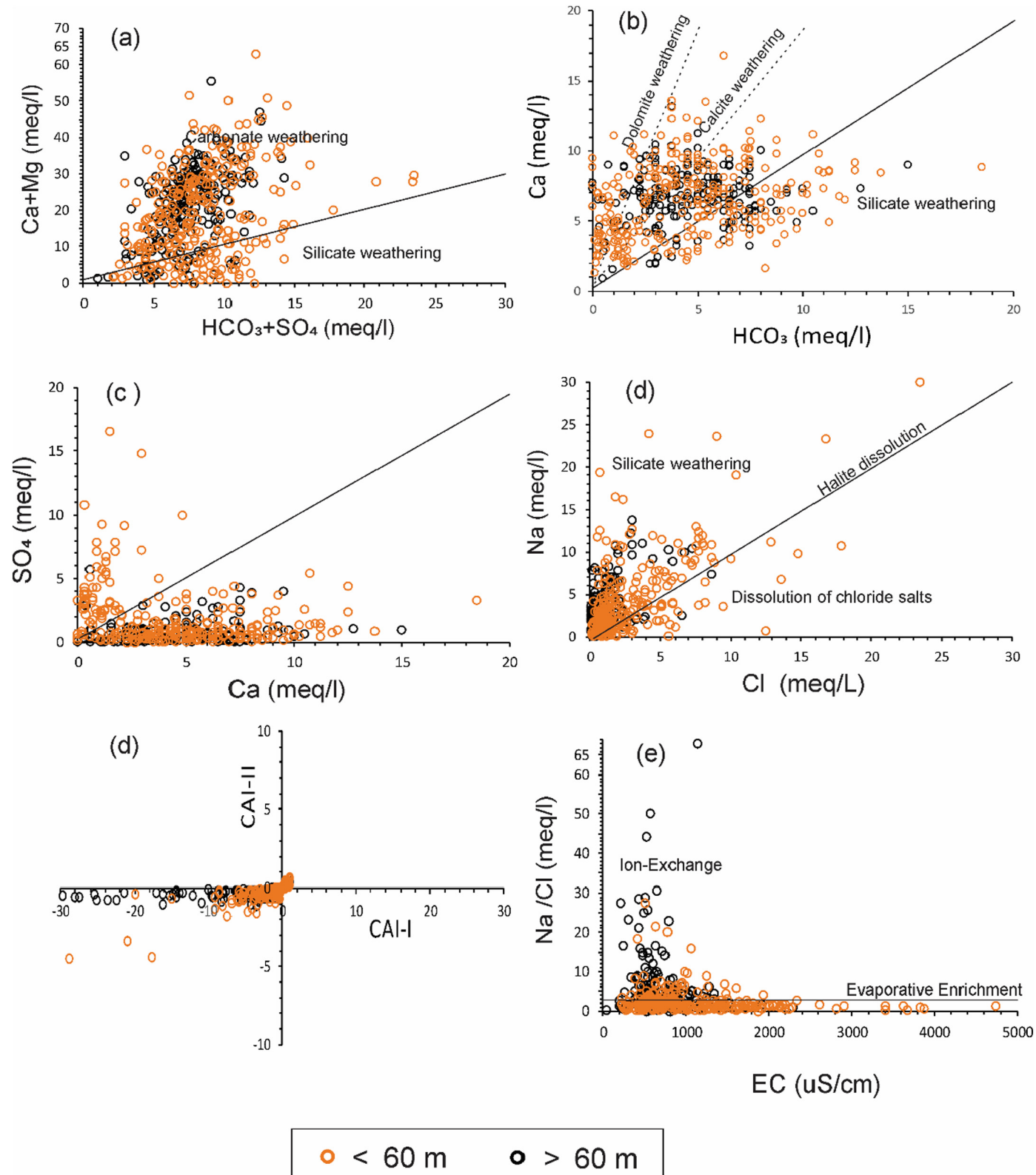


Fig. 4. Plots showing (a) $(\text{Ca}^{2+} + \text{Mg}^{2+})$ vs. $(\text{HCO}_3^- + \text{SO}_4^{2-})$, (b) Ca^{2+} vs. HCO_3^- , (c) SO_4^{2-} vs. Ca^{2+} , (d) Na^+ vs. Cl^- , (d) CAI-I vs. CAI-II and (e) Na^+/Cl^- vs. EC in shallow (<60 m) and deep (>60 m) groundwater of Punjab to understand the hydrochemical processes governing groundwater chemistry. (Chloro Alkaline Indices CAI-I and CAI-II are calculated in meq/L).

The abundance of Ca^{2+} , Mg^{2+} , and HCO_3^- and their good positive correlations in both groundwaters ($\rho = 0.34$ to 0.5; Table 2) indicates the prevalence of carbonates such as calcite and dolomite (Das et al., 2018). This can be further seen in the plot of $(\text{Ca}^{2+} + \text{Mg}^{2+})$ vs. $(\text{HCO}_3^- + \text{SO}_4^{2-})$ (Fig. 4a),

which shows most of the data are placed in the $\text{Ca}^{2+} + \text{Mg}^{2+}$ over $\text{SO}_4^{2-} + \text{HCO}_3^-$, indicating that carbonate weathering is a more predominant hydro-geochemical process and the major source of Ca^{2+} and Mg^{2+} in the groundwater (Kumar et al., 2009). This can be also seen in the Ca vs.

Table 2

Spearman's Rank correlation coefficients for hydrochemical parameters in shallow and deep groundwater of Punjab, India. This synthesis is based on data from 12 districts of Punjab (for details, see Supplementary Note 1).

	U	pH	EC	TDS	ORP	SL	DO	F ⁻	Cl ⁻	NO ₃ ⁻	SO ₄ ²⁻	PO ₄ ³⁻	HCO ₃ ⁻	Na ⁺	K ⁺	Ca ²⁺	Mg ²⁺	Fe
Shallow groundwater (<60 m)																		
U	1.00																	
pH	0.02	1.00																
EC	0.573*	-0.273*	1.00															
TDS	0.601*	-0.279*	0.997*	1.00														
ORP	-0.294*	-0.235*	-0.512*	-0.488*	1.00													
SL	0.50*	-0.240*	0.986*	0.982*	-0.220*	1.00												
DO	-0.05	0.362*	-0.346*	-0.344*	0.340*	-0.09	1.00											
F ⁻	0.501*	0.05	0.588*	0.636*	-0.576*	0.394*	-0.296*	1.00										
Cl ⁻	0.504*	-0.246*	0.719*	0.771*	-0.297*	0.561*	-0.214*	0.541*	1.00									
NO ₃ ⁻	0.427*	-0.218*	0.429*	0.445*	0.01	0.477*	0.10	0.223*	0.456*	1.00								
SO ₄ ²⁻	0.299*	-0.230*	0.570*	0.611*	-0.355*	0.292*	-0.355*	0.478*	0.561*	0.152	1.00							
PO ₄ ³⁻	-0.10	0.190	-0.07	-0.08	0.07	0.178	0.187	-0.10	-0.244*	-0.140	-0.17	1.00						
HCO ₃	0.375*	-0.206*	0.167	0.193*	0.383*	0.776*	0.133	0.105	-0.01	0.199	-0.17	0.318*	1.00					
Na ⁺	0.473*	-0.04	0.545*	0.567*	-0.244*	0.470*	-0.08	0.356*	0.510*	0.294*	0.253*	-0.03	0.160*	1.00				
K ⁺	0.363*	-0.184	0.336*	0.367*	-0.128	0.10	-0.152	0.324*	0.421*	0.188	0.319*	-0.380*	-0.11	0.452*	1.00			
Ca ²⁺	-0.09	-0.05	-0.263*	-0.264*	0.523*	0.153	0.414*	-0.384*	-0.11	0.191	-0.25*	0.191	0.362*	-0.151	-0.223*	1.00		
Mg ²⁺	-0.01	-0.258*	-0.06	-0.05	0.570*	0.446*	0.254*	-0.10	0.03	0.236*	-0.08	0.08	0.500*	-0.12	-0.03	0.45*	1.00	
Fe	-0.484*	-0.241*	-0.267*	-0.275*	0.424*	-0.288*	-0.337*	-0.188	-0.140	-0.32*	0.139	-0.05	-0.05	-0.37*	-0.148	-0.05	0.153	1.00
Deep groundwater (> 60 m)																		
U	1.00																	
pH	0.04	1.00																
EC	0.499*	-0.221*	1.00															
TDS	0.511*	-0.194	0.999*	1.00														
ORP	-0.05	-0.369*	-0.163	-0.147	1.00													
SL	0.490*	-0.178	0.996*	0.995*	-0.164*	1.00												
DO	-0.03	0.302*	-0.148	-0.13	0.04	-0.12	1.00											
F ⁻	0.257*	0.07	0.13	0.10	0.201*	0.07	0.01	1.00										
Cl ⁻	0.355*	-0.01	0.578*	0.618*	-0.05	0.597*	0.11	-0.07	1.00									
NO ₃ ⁻	0.178*	-0.187	0.377*	0.360*	0.08	0.390*	0.12	0.212*	0.270*	1.00								
SO ₄ ²⁻	0.279*	0.00	0.416*	0.435*	0.08	0.383*	0.05	0.252*	0.419*	0.142	1.00							
PO ₄ ³⁻	-0.01	0.05	0.07	0.06	-0.05	0.09	0.05	-0.05	0.01	-0.02	0.05	1.00						
HCO ₃	0.434*	-0.277*	0.661*	0.671*	0.09	0.720*	-0.186	0.212*	0.288*	0.281*	0.172	0.09	1.00					
Na ⁺	0.468*	0.145	0.441*	0.474*	-0.10	0.460*	-0.02	0.233*	0.317*	0.161	0.364*	0.01	0.326*	1.00				
K ⁺	0.424*	-0.156	0.176	0.161	0.437*	0.13	-0.01	0.211*	0.143*	0.285*	0.167	-0.10	0.284	0.387*	1.00			
Ca ²⁺	0.04	-0.143	0.140	0.10	0.180	0.14	0.06	-0.06	0.235*	0.353*	0.137	-0.05	0.34*	0.05	0.12	1.00		
Mg ²⁺	0.333*	-0.284*	0.320*	0.302*	0.262*	0.336*	0.01	0.291*	0.196	0.388*	0.174	0.01	0.494*	0.08	0.318*	0.203*	1.00	
Fe	-0.369*	-0.217*	-0.184	-0.281*	0.469*	-0.300*	0.06	0.164	0.04	0.00	0.152	0.00	-0.09	-0.270*	0.00	0.187	0.172	1.00

* Correlations are significant at $p < 0.001$; SL: salinity; TDS: total dissolved solid; ORP: oxidation-reduction potential; EC: electrolytic conductivity; Values >0.8 indicate strong correlation, >0.5 to 0.8 indicates high correlation and <0.5 to 0.34 denotes moderate correlation.

HCO_3^- plot (Fig. 4b). Moreover, several samples have higher concentrations of Mg^{2+} than Ca^{2+} , which may be due to reprecipitation of Ca^{2+} (Hem, 1985) or congruent dissolution of Mg-bearing carbonate minerals such as dolomites that commonly forms in arid/semi-arid regions under high evaporation and low rainfall conditions (Rashid et al., 2018). The latter hypothesis is supported given the saturation of dolomite (SI values up to 2) over calcite (Fig. 3d). In addition, the presence of kankar in these soils is an indicator of secondary carbonate precipitation. Mg^{2+} may also have been contributed from chemical fertilizers as most of the sampling locations are associated with agricultural land use (Keesari et al., 2014). Na^+ was one of the most abundant cation in the groundwater: the Na^+ vs Cl^- plot (Fig. 4d) shows that significant numbers of the samples fall above the 1:1 equiline, signifying that Na^+ may be attributed to silicate weathering (e.g., albite) and/or resulted from ion exchange processes as divalent cation can replace with monovalent cation in groundwater (Rajmohan and Elango, 2003; Luo et al., 2018), while samples below the 1:1 equiline indicate dissolution of chloride salts from the soil due to water level rise and/or mixing with canal water and increases in Cl^- may also be derived from other sources like fertilizers, domestic effluents, septic tanks, etc. (Kumar et al., 2009; Nasher and Ahmed, 2021). The molar ratios of $\text{Na}^+/\text{Cl}^- = 1$ in a significant number of samples reflects the congruent dissolution of halite (contributing Na^+), which can be supported by the positive correlation between Na^+ and Cl^- and by the fact that this relationship is stronger in shallow ($\rho = 0.51$) than deep aquifers ($\rho = 0.32$), which suggests that soluble salts (that usually form in arid/semiarid environment) are washed out and discharged to shallow aquifers. But, when the Na^+/Cl^- ratio > 1.5 indicates incongruent dissolution of Na^+ bearing silicate minerals like feldspar as the source of Na^+ (Kumar et al., 2014). In the plot of Na^+/Cl^- vs. EC (Fig. 4e), Na^+/Cl^- showed a decreasing trend with increasing EC wherein higher ratios of Na^+/Cl^- indicate that the Na^+ originated from the silicate weathering or ion exchange, while lower ratios with increasing EC indicating the role of evaporative enrichment to increase Na concentration in groundwater. The role of ion exchange as a process for Na^+ enrichment in groundwater was determined by Chloro-Alkaline Indices (CAI; Schoeller, 1967); in which positive values of CAI-1 and CAI-2 indicates base exchange between Na^+ or K^+ with Mg^{2+} or Ca^{2+} , while negative values of both indices indicate reverse ion exchange processes (Schoeller,

1967). In our study, more than 75% of the groundwater samples have negative values of both CAI-1 and CAI-2 (Fig. 4d), suggesting a reverse ion exchange or dominance of cation exchange process in the aquifer system. This is corroborated by Kumar et al. (2009). In this process, Ca^{2+} and Mg^{2+} ions in the groundwater are exchanged with Na^+ and K^+ from the host-rocks.

HCO_3^- is a dominant anion in the groundwaters; its major source is the chemical weathering of carbonate and silicate aquifer host rocks (Keesari et al., 2014). The formation of HCO_3^- in this agri-intensive region is due to infiltration of irrigated water that results in the dissolution of carbonate minerals along the path, and release of bicarbonate into the groundwater. Also, inputs of agrochemicals, decaying organic matter, and root respiration significantly increase the amount of CO_2 (g) in agricultural soils which reacts with pore water to form H_2CO_3 that dissociates readily to form HCO_3^- . Enrichment of SO_4^{2-} in groundwater can come from either oxidation of sulfide minerals, or weathering/dissolution of gypsum ($\text{CaSO}_4 \cdot 2\text{H}_2\text{O}$) in aquifer rocks and sediments, or SO_4^{2-} bearing agrochemicals (Ritzi et al., 1993; Nasher and Ahmed, 2021). Oxidation of sulfide is unlikely in both water types due to poor correlation between Fe and SO_4^{2-} ($\rho = 0.13$ to 0.15). For SO_4^{2-} vs Ca^{2+} plots (Fig. 4c), approximately 50% of the samples have $\text{Ca}^{2+}:\text{SO}_4^{2-} > 1$, indicating a significant amount of gypsum in the study area (Purushothaman et al., 2014). Contrary, no samples fell along the equiline (1:1) suggesting less probability of a CaSO_4 (anhedral) as a source (Kumar et al., 2019). This is corroborated by the SI results (Fig. 3d).

4.3. Uranium distribution in groundwater

The distribution of U in the groundwater of all 23 districts is shown in Fig. 1c and Table 1, which show that U concentrations strongly vary with depth with significantly higher concentrations ($0.15 \mu\text{g l}^{-1}$ to $476 \mu\text{g l}^{-1}$) and larger quartile values in the shallow groundwaters compared to deep waters (0.02 to $275 \mu\text{g l}^{-1}$). U contamination varied spatially with the highest levels occurring in the southwestern districts of the Malwa belt (Fig. 1c). Districtwise U levels exceed WHO guidelines ($30 \mu\text{g l}^{-1}$) in as high as 81% of the samples from the 9 districts located in southern and southwest areas of Malwa Region (Table 3; Fig. S2). The top 5 most affected districts include Barnala (81% samples exceeding WHO guidelines), Moga

Table 3

District-wise uranium statistics (concentration in $\mu\text{g l}^{-1}$) and percentage of samples exceeding WHO guideline value for drinking purpose (WHO, 2017) in groundwater of Punjab.

Districts	TN	Min	Mean	Med $\mu\text{g l}^{-1}$	Q1	Q3	Max	Samples > WHO limit	
								N	%
Tarn Taran	126	0.02	16.4	8.7	2.1	20.57	156.9	19	15.08
Pathankot	47	0.2	1.778	0.5	0.2	1.275	41.1	1	2.17
Amritsar	483	0.1	6.334	4.3	1.5	9.5	196	2	0.41
Gurdaspur	138	0.1	2.842	1.15	0.3	3	32	1	0.72
Nawashaher	51	0.15	16.71	14.8	6.01	25.55	65.04	6	11.76
Kapurthala	13	1.93	22.14	19.29	7.62	22.02	107	1	7.69
Jalandhar	22	3.54	21.59	16.33	10.85	27.81	66.65	3	13.64
Hoshiarpur	20	0.9	7.09	6.59	1.55	10.7	19.79	0	0.00
Barnala	49	0.88	53.92	42.72	32.67	63.25	131.2	40	81.63
Patiala	99	0.7	22.88	15.8	7.98	27.8	267	21	21.21
SBS Nagar	41	0.15	15.38	11.77	5.69	20.84	65.04	5	12.20
Sangrur	137	1	51.63	37.6	23.72	68.36	230.3	80	58.39
Rupnagar	66	0.29	7.04	4.29	2.18	7.98	46.3	3	4.55
Ferozpur	159	0.5	43.69	27.5	14.23	68	331.42	70	46.05
Fazilka	82	1.3	65.75	44.35	21.03	99.17	277.6	51	62.20
Muktsar	22	5	37.55	28.2	11.6	51.91	149.7	9	40.91
Moga	195	0.1	79.31	69.7	35.5	103.1	348	150	76.92
Mansa	25	7.2	70.3	31.1	20.5	68	379	14	56.00
Ludhiana	151	0.5	19.2	17	9.3	26	71.1	24	15.89
SAS Nagar	23	0.4	14.77	6.7	3.6	10	193.3	1	4.35
Bathinda	49	3	94.8	65.7	38	135.7	432	38	77.55
Fatehgarh	52	1	28.66	24.68	14.1	37.35	126	19	36.54
Faridkot	11	0.6	157	123	12.7	299.7	476.5	8	72.73
Total	2062	0.1	30.01	12.5	3.72	34.52	476.5	564	27.37

TN: total number of samples; 'N' and '%' depict number and percentage of samples exceeding WHO guideline value for drinking water ($30 \mu\text{g l}^{-1}$), respectively; Min: minimum; Max: Maximum; Med: Median; Q1 and Q3 are lower and upper quartiles, respectively.

(77%), Bathinda (76%), Fazilka (62%), and Faridkot (72%). Based on the AERB limit ($60 \mu\text{g l}^{-1}$), the most affected districts in Punjab are Moga (65%), followed by Faridkot (63%), Bathinda (55%), and Fazilka (45%), while all other districts were <35%. This is corroborated by previous studies (Table S1), which show that more than 80% of the occurrence of U is from districts in the Malwa Region, namely Bathinda, Mansa, Barnala, Fazilka, and Ferozpur. The highest concentration of U ($1340 \mu\text{g l}^{-1}$) is reported in the groundwater of Mansa district (Sharma and Singh, 2016). Bathinda district is the most studied and has the third-highest level of U ($644 \mu\text{g l}^{-1}$) (Kumar et al., 2011b) and highest number of cancer cases in Punjab. In this district, the concentration of U exceeds WHO limits in 42–85% of the samples, which is similar to Mansa and Faridkot districts. Districts falling in the Majha and Doaba belts of Punjab record lower concentrations of U compared with the districts of Malwa belt (Fig. 1c, Table 3).

4.4. Geochemical factors controlling U mobilization

U speciation and mobility are linked to the presence of multiple elements/compounds which occur simultaneously in groundwater (Bonotto et al., 2019). Our primary focus was to understand the interrelationships between these variables and how they govern the U behavior in the aquifers with emphasis on pH, EC, TDS, Salinity, ORP, NO_3^- , HCO_3^- , Na, Cl^- , SO_4^{2-} , Ca, Mg, Fe. The relationship between U and other parameters was evaluated based on the Spearman's Rank correlation coefficients (Table 2), speciation analysis (Fig. 3e), and bivariate plots (Fig. S3).

4.4.1. Effect of EC, TDS, salinity, Na^+ and Cl^-

U is more strongly correlated with TDS ($\rho = 0.6$), EC ($\rho = 0.57$), salinity ($\rho = 0.49$), Na^+ ($\rho = 0.47$), and Cl^- ($\rho = 0.5$) in shallow groundwater than deep groundwater (U-TDS, $\rho = 0.51$; U-EC, $\rho = 0.49$; U-salinity, $\rho = 0.49$; U- Na^+ , $\rho = 0.46$; U- Cl^- , $\rho = 0.35$) (Table 2; Fig. S3). These parameters are also more predominant in shallow groundwaters (Table 1; Fig. 2). The strongest relationship was observed between U and TDS (Table 2; Fig. S3), indicating that U mobility in groundwater sharply increases with increasing TDS. The most likely source of high TDS is from saline groundwater as shown by the strong relationship of TDS with salinity, Na and Cl^- (Table 2), which is largely a function of sediment-water interaction, dissolution of salts/evaporite minerals, excessive irrigation recharge, and addition of nutrients from mineral fertilizers. The contribution of irrigation recharge which results in the mixing of canal and groundwater is confined to the shallow aquifer (Krishan et al., 2021). As a result, there is a greater mobilization of U in shallow aquifers relative to deeper aquifers. This effect can be seen by an increased TDS and U in the groundwater which is accompanied by a change towards more mixed water facies; U concentrations rise with increasing Na-Cl, Mg-Cl and Na-HCO₃ facies (Fig. 3c). Other reasons, which can be linked to salt precipitation as a result of high rates of evaporation and low precipitation such as the arid/semi-arid conditions, play an important role in increasing the TDS/salinity level (Alcaine et al., 2020; Krishan et al., 2021; Smedley et al., 2002). The effect of TDS (a major factor in salinity) on the mobility of U indicates that high salt content is the main factor in controlling U contamination in the shallow groundwater. The most plausible explanation for high salt/TDS induced U mobilization is the increase in ionic strength and major ions which decrease adsorption of dissolved U species through high competition between ions and mobilized U from soil exchange sites/other mineral surfaces through ion exchange mechanisms (Li et al., 2016; Rout et al., 2015; Sturchio et al., 2001). Also, increases in salt concentrations result in the formation of soluble U-complexes that are the key drivers of U solubility in aquifers (Rout et al., 2015). U enrichment associated with high TDS in the arid environment was also reported from UAE by Xiong et al. (2020) and Rout et al. (2015) showed that at high salinity a significant amount of U was released from soil. In contrast, at low TDS, mobile U is strongly adsorbed on minerals surfaces due to less competition between ions (Kumar et al., 2014). It is also well known that UO_2^{2+} (VI) is less mobile in water and strongly adsorbed on Feoxydioxide/clay minerals and organic surfaces when there is less

competition in low ionic strength waters. Thus, adding salts to groundwater can have a strong positive effect on U mobilization (Drage and Kennedy, 2013; Riedel and Kubeck, 2018).

4.4.2. Effect of HCO_3^- , pH and, ORP

In U prone areas, aquifers under oxidizing and alkaline conditions typically have high U values due to the occurrence of HCO_3^- (Wu et al., 2014). Alkaline pH (>7) leads to the dissolution of U in water (Wu et al., 2014) and reduces the adsorption due to its effect on the speciation of U(VI) and the surface charge of the functional groups (Li et al., 2016). While, higher ORP results in the predominance of more mobile U(VI), reducing conditions favor the less mobile U(IV) (Riedel and Kubeck, 2018). In this study no clear vertical (Fig. 2) or lateral (Fig. S3) trend was found between pH, ORP and U; a weak negative correlation was noted between U and the dissolved oxygen (DO) (Table 2). This shows that pH and ORP are not significant factors controlling U behavior. However, the groundwaters are mostly oxic and alkaline in nature throughout the region. This is attributed to their shallow depths and sandy textures with an admixture of gravel, sand, and silt with varying proportions of kankar. Anthropogenic influences, including groundwater abstraction, and surface-groundwater interactions (leaking irrigation) also lead to drawdown and result in oxic conditions. When the conditions are both oxic (positive ORP) and alkaline ($\text{pH} > 7$) environment, U is more likely to form uranyl ions (UO_2^{2+}) which form soluble uranyl-carbonate complexes (Wu et al., 2014). Because these anions do not readily adsorb to mineral surfaces at basic pH, these carbonate species may facilitate the desorption of U from mineral surfaces. Also, competition of HCO_3^- with U oxyanions for sorption sites of Fe-oxides/oxyhydroxides results in U mobility (Clark et al., 1995; Wu et al., 2014). This is evidenced by the positive relation between U and HCO_3^- (Table 2; Fig. S3). This is also consistent with speciation modeling (Geochemist Workbench), which showed the predominance of uranyl-carbonate species $\text{UO}_2\text{CO}_3^{2-}$ and $\text{UO}_2\text{CO}_3^{3-}$ (Fig. 3e), which together constitute >95% of the total dissolved U. Similar speciation results have been previously reported elsewhere in similar groundwaters (Krestou and Panias, 2004; Kumar et al., 2014; Wu et al., 2014; Coyte et al., 2018; Cao and Choo, 2019). However, these studies reported that the HCO_3^- is the most predominant controlling parameter for U (Coyte et al., 2018), while in this study TDS/salinity remained the principal factor of U mobilization, followed by HCO_3^- . Other complexes such as U-Cl and U-SO₄ can influence U mobility, but this is less likely due to their low abundance in groundwaters (Fig. 5b). Furthermore, under oxidizing and carbonate dominating conditions, U could easily form complexes with Ca^{2+} as $\text{HCO}_3^-(\text{Ca}_2\text{UO}_2(\text{CO}_3)_3^{2-})$ and $\text{CaUO}_2(\text{CO}_3)_3^{2-}/\text{UO}_2(\text{CO}_3)_3^{4-}$ (Wu et al., 2018). The first complex contributes to more U mobility as it is less likely to adsorb and is not bioavailable to the U-reducing bacteria (Stewart et al., 2011). However, high evaporation and increased salinity under arid/semi-arid conditions encouraged removal of Ca via precipitation of calcite (Luo et al., 2018). This may be one of the processes responsible for U immobilization in some waters (Catalano et al., 2006), and is supported by the negative correlation between U and Ca and absence of Ca-bearing U species.

4.4.3. Effect of NO_3^-

Nitrate impacts the U behavior in groundwater owing to its oxidizing properties, which leads to the oxidative dissolution of U(IV) bound to Fe/Mn oxides and organic matter (Bonotto et al., 2019; Rout et al., 2015). NO_3^- also competes with U(VI) species for exchange sites in high ionic strength solutions, resulting in higher U mobility (Dong and Brooks, 2008). NO_3^- concentrations in this study are higher in shallow groundwaters than in deeper ones (Fig. 2), and also it is better correlated with U in shallow water ($\rho = 0.47$) than deep water ($\rho = 0.17$) (Table 2). This indicates that shallower wells are more susceptible to U contamination as they are more likely to have higher NO_3^- from agricultural runoff. Previous studies have also reported that the NO_3^- presence may increase the U mobility (Bonotto et al., 2019; Cumberland et al., 2016; Riedel and Kubeck, 2018). However, despite having high NO_3^- concentrations in some deep water samples, they are low in U (Fig. 2), exhibiting a negative correlation

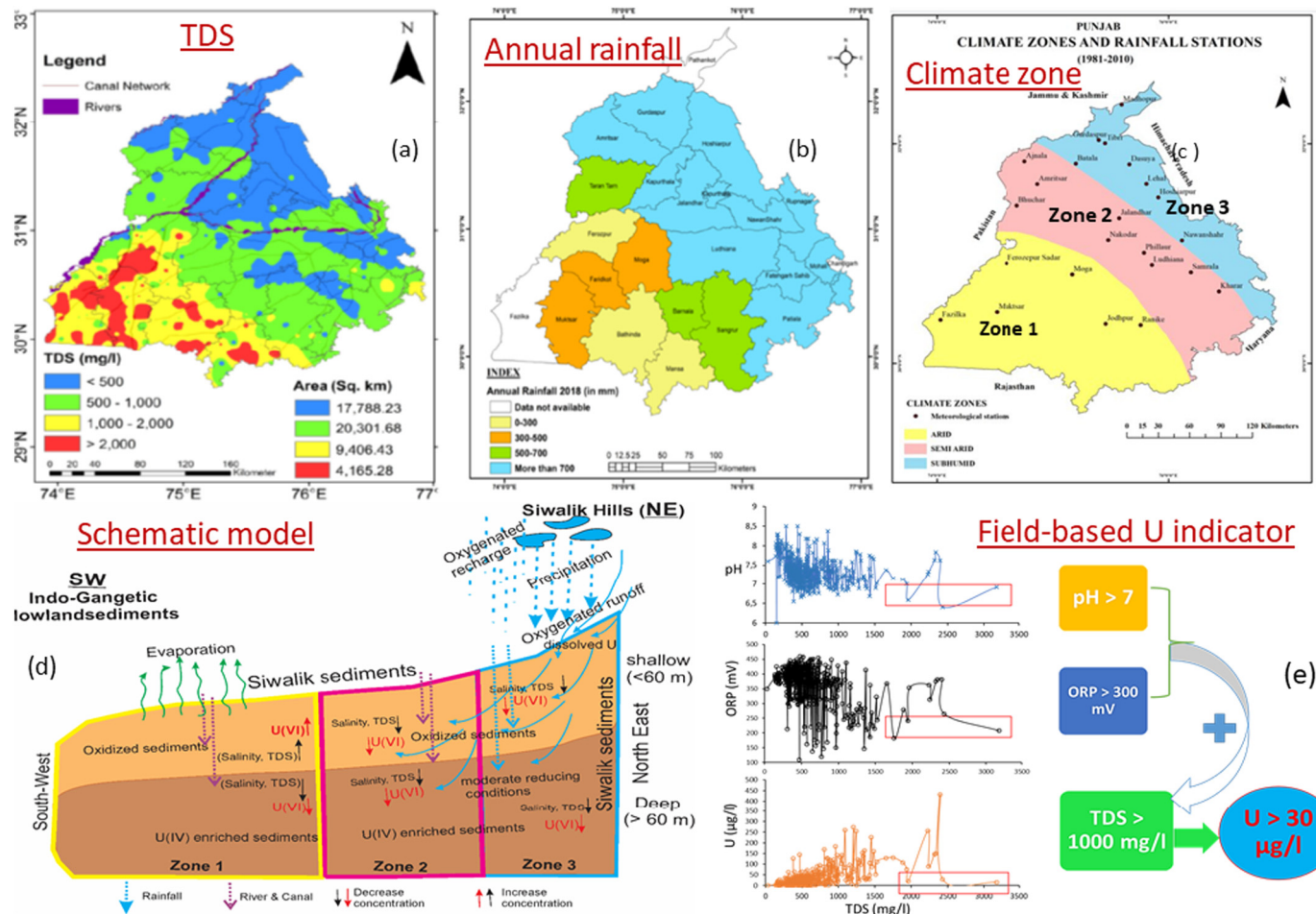


Fig. 5. (a) Distribution of total dissolved solids (TDS) in groundwater (modified from Krishan et al., 2021); (b) district-wise south west monsoon annual rainfall pattern during 2018 (CGWB, 2021); (c) climatic zones of Punjab (Sharma and Singh, 2017); (d) schematic representation showing the geogenic provenance of U and depth wise U, TDS, salinity, and redox conditions along with major recharge sources and evaporation process in the three zones of Punjab that control solubility and mobility of U in groundwater (modified from Krishan et al., 2021); and (e) TDS-pH-ORP (ORP: oxidation-reduction potential) relationship to predict U levels in groundwater above the WHO guideline value of $30 \mu\text{g l}^{-1}$ (please see text for explanation).

(Table 2). This may be due to the relatively reducing conditions at depth, as indicated by higher amounts of Fe. Furthermore, high NO_3^- and low Fe in shallow groundwater support the hypothesis for oxidizing conditions in the shallower U-rich groundwater. Thus, a nitrogen fertilizer usage, where the groundwater is highly oxidizing, is more likely to contribute to increased U concentrations; however, prevailing redox conditions are important when accounting for NO_3^- dependent U mobility. Moreover, a few samples with high NO_3^- concentrations in the deeper part of the aquifer indicates vulnerability to vertical migration of anthropogenic contaminants, which may be due to intensive groundwater abstraction from deeper aquifers (Lapworth et al., 2017).

4.4.4. Effect of Fe , SO_4^{2-} , and PO_4^{3-}

Fe-oxyhydroxides strongly adsorb UO_2^{2+} due to their high specific surface areas and high binding affinity (Payne et al., 1996). The negative correlation between U and Fe (Table 2) may indicate U(VI) immobilization by sorption onto Fe-oxyhydroxides (goethite) (Grybos et al., 2007). Alkaline and oxic environments also favor Fe^{3+} adsorption through complexation with OH^- and the formation of secondary Fe(III) oxides/hydroxides. This is evident as groundwaters in the study area are mostly supersaturated with respect to goethite (SI value 4 to 6; Fig. 3d). The high Fe content in deeper water indicates dissolution of Fe(hydr)oxides under reducing conditions, which could potentially increase the level of U; however, under those conditions the released U would tend to re-precipitate and immobilize, resulting in low U (Wu et al., 2014). Moreover, under reducing conditions,

the adsorbed U(VI) can be readily reduced by the production of FeS_2 and FeCO_3 , in the presence of S^{2-} and Fe^{2+} (Veeramani et al., 2013), which could be the cause of low U in deeper aquifers (Wu et al., 2018). However, as shown in the vertical distribution plots (Fig. 2), SO_4^{2-} is enriched in the shallow aquifers while Fe is enriched in deeper water, and they are poorly correlated in deep water (Table 2). Thus, sulfide formation may not be favored. Moreover, the moderate correlation between U and SO_4^{2-} ($\rho = 0.27$ to 0.29) in both waters indicate that SO_4^{2-} may facilitate the U mobilization via competing with oxyanion U-species.

PO_4^{3-} can play an important role by forming U- PO_4 complexes in an alkaline environment (Seder-Colomina et al., 2015a; Seder-Colomina et al., 2015b). However, in our study, PO_4^{3-} is 3 to 4 orders of magnitude lower than HCO_3^- , so it is unlikely that it can compete with carbonate to form aqueous U (VI) phosphate complexes; this is evidenced in the speciation data (Fig. 3e). Furthermore, the presence of PO_4^{3-} is also attributed to the formation of goethite-associated uranyl-phosphate- Fe(III) complexes and/or uranyl-phosphate-clay complex under oxidizing conditions that are more stable than the adsorbed U species formed in the absence of phosphate (Del Nero et al., 2011; Finch and Murakami, 1999; Seder-Colomina et al., 2015a; Seder-Colomina et al., 2015b). Wu et al. (2014) also showed that PO_4^{3-} could potentially decrease U(VI) solubility by adsorption/precipitation of low solubility U(VI)-phosphates in soils. Cheng et al. (2004) also studied the role of PO_4^{3-} on U(VI) adsorption to goethite and Jerden and Sinha (2003) reported PO_4^{3-} based immobilization of uranium in an oxidizing bedrock aquifer. However, in our study, PO_4^{3-} is very weakly

correlated with U (**Table 2**; Fig. S3). Furthermore, considering the very low concentrations of PO_4^{3-} in groundwater, it is unlikely that P-fertilizers are the source of U contamination in the Malwa Region ([Alrakabi et al., 2011](#)).

4.4.5. Effect of co-contamination of F^- and U

Fluoride is significantly positively correlated with U (p -value <0.001), with a stronger correlation in shallow ($\rho = 0.51$) than deep aquifers ($\rho = 0.25$) (**Table 2**). This strong co-occurrence and their significantly higher concentrations in the shallow aquifers may be due to common origin or similarities in their preferred environment and groundwater chemistry that control metal mobility ([Das et al., 2018](#)). Typically, the mobility of F^- is increased in alkaline pH (pH 7 to 9) with a relatively high concentration of NaHCO_3 , and low Ca water ([Brunt et al., 2004](#); [Das et al., 2018](#)). However, the weak correlation between F^- and Na ($\rho = 0.35$) and F^- and HCO_3^- ($\rho = 0.1$) and comparatively higher positive correlation between F^- and salinity/TDS ($\rho = 0.63$) in shallow aquifers indicates that the F^- mobility is highly influenced by groundwater salinity, similar to U. Considering this result, the salt effect is critical for controlling co-contamination of U and F in the study area. In fact, this observed relation agrees with some previous studies which mentioned high EC/TDS along with alkaline conditions as reasons for high F^- in groundwater ([Abiye and Shaduka, 2017](#)). Also, the co-occurrence of these oxyanion-forming elements is strongly influenced by environment and climatic conditions ([Kumar et al., 2020a](#)). [Das et al. \(2018\)](#) and [Das and Kumar \(2018\)](#) noted that the co-occurrence of U, As, and F^- in aquifers in arid/semi-arid regions with oxidizing conditions, could favor higher solubilities as the environment favored water-rock/sediment interactions. Similar reasons are given for the co-existence of U, F^- , As and other co-contaminants in groundwaters of arid and/or semi-arid regions in La Pampa province (Eduardo Castex) ([Alcaine et al., 2020](#); [Smedley et al., 2002](#)), also in Santiago del Estero, Argentina ([Bundschuh et al., 2004](#)), Latin America ([Alarcón-Herrera et al., 2013](#)), and Namakwaland, South Africa ([Makubalo and Diamond, 2020](#)). While all these works present common findings, a better understanding of the geochemical processes resulting in the co-occurrence of these contaminants in the Punjab basin is required.

4.5. Multivariate analysis

The PCA method was used to further evaluate the contribution of different hydrogeochemical processes and determine the key factors responsible for U contamination in groundwater. Three principal components (PC), with Eigenvalues >1 , were identified, accounting for 61% of the total variance (**Table S5**), and elucidated interesting hydrogeochemical trends. The PCA biplot (Fig. S4a) shows the strong relationship between TDS, EC, salinity, Na^+ , Cl^- , HCO_3^- , F^- and U, which are largely related to PC1 (accounting for 41% of the total variance), indicating their control on hydrochemical parameters responsible for U contamination in groundwater. Also, U plus TDS, F^- , Cl^- and NO_3^- occur in one cluster and are highly correlated (**Table 2**), indicating the influence of both geogenic and anthropogenic processes. The second PC (with 12% variance) shows that Fe and ORP exert negative loading, while ORP and DO are negatively loaded on PC 3 (accounts for 7% of variance). Interestingly, the same cluster was identified in the HCA results (Fig. S4b), particularly with the association of U with TDS and salinity. This result further provides a strong evidence of the role of TDS/salinity in U mobilization. Also, the HCA study identified the important relationships between hydrogeochemical parameters, especially the correlation of anions with TDS, salinity and U, which was not shown by PCA analysis. This indicates that major anions play a more significant role in U solubilization, which could be explained by their more competitive reactions with the oxyanion uranyl-carbonate species. The increasing trend in Cl^- bearing facies (like Mg-Cl, Na-Cl, etc.; **Fig. 3c**) with increasing U support this observation. This was also corroborated by [Riedel and Kubeck \(2018\)](#).

4.6. Possible cause of U contamination in the Malwa region

Malwa region is the hot spot for U contamination: a very large number of samples from several districts exceed the WHO permissible limit ($30 \mu\text{g l}^{-1}$) as well as the Atomic Energy Regulatory Board (AERB) limit ($60 \mu\text{g l}^{-1}$) (**Table 3**; Fig. S2). Considering the fact that high TDS/salinity is the predominant cause of U contamination, it is important to understand the cause of high TDS in the Malwa region. The high TDS in southwest Punjab is well correlated with arid-climatic conditions and low precipitation (**Fig. 5a, b, c**). Arid conditions result in the precipitation of evaporites and increased salts/TDS level in groundwater in consequence of high rates of evaporation and low precipitation. These factors are inversely related to the percentage of samples with U levels exceeding the WHO permissible limit across all Punjab districts (Fig. S5). Other reasons are that the depth to the water table decreases towards the southwest and that there are high water table fluctuations in this region (Fig. S1) due to over-pumping of groundwater for agriculture. This may result in infiltration of saline water into fresh groundwater (mixing) and ultimately increasing salinity and oxidizing conditions. In addition, the formation of bicarbonates due to the percolation of carbonic-rich water through Ca-rich soils would facilitate U mobility. All these factors increase TDS/EC, salinity, HCO_3^- , and oxic conditions, and may be the main reasons responsible for the unusual high U contamination in the Malwa region.

The origin of U in the Punjab basin is U-rich sediments from the Himalayas ([CGWB, 2020](#); [Patnaik et al., 2016](#)). We have created a conceptual model to help understand U occurrence and distribution in the basin (**Fig. 5d**), which we divided into three zones. These zones are based mainly on differences in topography, hydrogeology, and climate, which subsequently control ORP-alkalinity-salinity. Overall, groundwater flow is from the NE towards the SW. Zone 3 is located in the north and northeast, semi-humid, high rainfall part of the basin. The high rainfall which recharges groundwater resources dilutes the TDS/salinity level in this area ([Krishan et al., 2021](#)). This factor results in the lowest U concentration of the 3 zones. Zone 2, towards the middle of the basin, is semi-arid with moderate salinity and where there is a mixture of canal and groundwater and still significant rainfall, leading to moderate U occurrence. In zone 1, at the southwestern part of the Punjab basin, the conditions are arid with low rainfall, high evaporation, shallow water table and higher agricultural activity. These factors result in higher redox and significantly increase TDS/salinity levels ([Krishan et al., 2021](#)), which favor U mobilization and resulted in higher U levels in this zone. The geochemical rationale for how these zones impact overall U occurrence and distribution are given in the above sections.

4.7. Field-based parameters as an indicator of U contamination

Geochemical relationships between U and other parameters indicate that TDS (which is mainly contributed by salinity) is the key driver that triggers U solubility in the alluvial aquifers of Punjab. While the majority of the samples follow this TDS-U relationship, a few samples do not (**Fig. 5e**), suggesting that there are other pertinent factors. Typically, samples with high TDS but low U are associated with low $\text{pH} < 7$ and low ORP values (approximately 119 to 250 mV). As the ORP decreases, it is presumed that the reducing intervals may be present which change of U species from U(VI) to U(IV). This can be seen in the stability diagram of U species which was constructed based on the average concentrations of U, SO_4^{2-} , HCO_3^- and Cl^- (**Fig. S6**). In anoxic waters (low redox potential; Eh (<200 mV; approximated by ORP) and acidic pH of < 6 , U stabilizes in the form of U_4O_9 (c) and uraninite, which have lower solubility and higher tendency to precipitate, whereas in oxidizing conditions (Eh > 200 mV) and alkaline pH ($\text{pH} > 7$), U(VI) species dominate in the form of carbonate complexes such as $\text{UO}_2(\text{CO}_3)_2^{2-}$ and $\text{UO}_2(\text{CO}_3)_2^{4-}$ (**Fig. S6**); these species were accounted for more than 95% of the total dissolved U (VI) in the studied groundwaters (**Fig. 3e**). Uranyl sulphate complexes as UO_2SO_4 and $\text{U}(\text{SO}_4)_2$ were formed at acidic pH ($\text{pH} < 6$). However, this had a minimum impact because the groundwaters of the study region are mostly alkaline

in nature. This clearly indicates that U solubility is highly dependent on pH and redox conditions. In this study, when TDS levels are $>1000 \text{ mg l}^{-1}$ along with $\text{pH} > 7$ and $\text{ORP} > 300 \text{ mV}$, U levels mostly exceeded the WHO drinking limit ($30 \mu\text{g l}^{-1}$) (Fig. 5e). This relationship demonstrates that the combination of all three field-based parameters, TDS along with pH and ORP, can be used as an indicator to evaluate preliminary risk assessment for U contamination for Punjab groundwaters. However, considering the limitation of the field parameters on both spatial and temporal scale, further studies are required to get more precise information to validate this relationship and formulate a field-based U-risk index.

4.8. Chemical toxicity risk of uranium on local residents

The chemical/non-carcinogenic health risk of U for local residents of Punjab through daily consumption of groundwater has been calculated as hazard quotient (HQ) following USEPA (US Environmental Protection Agency, 1989). The spatial distribution of U-health risks in both shallow and deep groundwaters of the Punjab State is given in Fig. S7. The non-cancerogenous risks exceeded the USEPA health risk limit ($\text{HQ} > 1$) in most of the Malwa Region where HQ ranged from 1.1 to 5.0 and in some patches the HQ range was exceptionally high ranging from 5 to 21. The local population of Bathinda, Moga and upper-middle parts of Mansa districts are facing significant risk due to chemica toxicity of U ($\text{HQ} 3-5$). Inhabitants of the northern parts of Punjab (Pathankot, Gurdaspur, Hoshiarpur, Tarn Taran, and Amritsar) and eastward districts (SBS Nagar and Rupnagar) face relatively low risks ($\text{HQ} < 1$). For the sake of comparison with U-concentration maps (Fig. 1c), the overall area of Malwa region has high groundwater U and it is well correlated with elevated health risks. This suggests that U concentrations in groundwater are one of the major factors for intensifying health problems. Previous studies of groundwater of the Malwa region have also reported high U-risk to local populations (Bajwa et al., 2017; Kaur et al., 2021; Kumar et al., 2020b; Kumar et al., 2021; Sharma and Singh, 2016).

5. Conclusions

The present study revealed that the Malwa region is the hot spot of U contamination in Punjab, in which the five most contaminated districts are Barnala, Moga, Bathinda, Fazilka, and Faridkot. U-based chemical/non-carcinogenic health risks are significant throughout the southwestern Punjab. Uranium is much more enriched in the shallower groundwater than the deep one. In general, groundwaters are oxic and alkaline in nature and the dominant hydrogeochemical facies were the Mg-HCO₃ type, but the species change more towards mixed water types (Na-Cl, Mg-Cl, and Na-HCO₃) when the U level increased - this is more evident in shallow groundwater. The groundwater chemistry of the study area is mainly controlled by carbonate weathering. Positive redox (ORP), alkaline pH, and dominating of HCO₃⁻ and U-carbonate complexes (UO₂CO₃²⁻ and UO₂CO₃³⁻) may contribute to the high solubility of U in groundwater. A strong positive correlation between U and TDS and salinity indicates that the salt effect is the main factor in controlling U contamination in the shallow groundwater. The most plausible explanation for the salt-induced U mobilization is related to an increased ionic strength of the solution and a high competition between ions for adsorption sites. NO₃⁻ also exhibits a positively correlation with U in shallow groundwater owing to its oxidizing properties. At conditions of [$\text{TDS} > 1000 \text{ mg l}^{-1}$ + $\text{pH} > 7$ + $\text{ORP} > 300 \text{ mV}$] the studied samples contained an excess amount of U with respect to the WHO permissible limits ($30 \mu\text{g l}^{-1}$). Thus, the combination of these field-based parameters can be used as a tool for preliminary risk assessment of U. The high U (and its co-occurrence with F⁻) in the Malwa region is likely due to a geogenic origin, but high salinity due to arid and semi-arid climatic and anthropogenic factors further influence mobility and enrichment. The high salinity in this region is largely a function of low rainfall and high evaporation in a hot and arid climate that promotes the precipitation of evaporite minerals (or salts). The

anthropogenic factors, especially the over-pumping of groundwater for agriculture irrigation, mixing of canal water with groundwater (which induced oxic and saline conditions), as well as the use of agro-chemicals (mainly nitrate fertilizers) are more prevalent in shallow aquifers and hence resulted in higher U contamination.

Overall, the present study highlights the key drivers of U contamination, and it lays the foundation for further studies in this direction. These may include source apportionment studies, investigation of the U distribution in core sediments and its leaching behavior, including adsorption/desorption experiments in presence of major cations and anions in similar environmental conditions, and quantification of the role of climatic variation factors, seasonal water table fluctuations, and agrochemicals/fertilizers in co-contamination of U and F⁻ in shallow aquifers. Solid evidence in this direction will be very helpful to implement preventive management practices to mitigate the U contamination problem in the alluvial aquifer of Punjab, India.

Supplementary data to this article can be found online at <https://doi.org/10.1016/j.scitotenv.2021.151753>.

CRediT authorship contribution statement

This review article was prepared by 10 authors with their following contributions.

Conceptualization, P.K.S, J.P., S.M, R.P.T; Data curation, P.K.S, H.S.V, R.K, L.C; Formal analysis, P.K.S, M.P; Methodology and Map preparation: G.N.S., R.K., Writing—original draft: P.K.S., M.P., Supervision: S.M., J.P. R.P.T, Writing—review & editing, H.S.V., J.P., S.M., G.N.S., Y.K.N. All authors have read and agreed to the published version of the manuscript.

Declaration of competing interest

The authors declare that there are no known conflicts of interest associated with this publication and there has been no significant financial support for this work that could have influenced its outcome. All of the sources of funding for the work described in this publication are acknowledged in the manuscript.

Acknowledgements

We thankfully acknowledge the authorities of PWSSD (Punjab Water Supply and Sanitation Department) for the supply of U data in groundwater for several districts of Punjab. We acknowledge the DIST-FIST (Fund for Improvement of S & T Infrastructure of the Department of Science and Technology) instrumentation laboratory at the Department of Environmental Science and Technology, Central University of Punjab, Bathinda, for providing support to this work. We also thankful to Prof. Abhijeet Mukherjee, IIT Kharagpur, for providing scientific input. We sincerely thank the Special-Issue Editors and four anonymous reviewers for their valuable suggestions and critiques, which have increased the scientific value of this manuscript by many folds.

References

- Abiye, T., Shaduka, I., 2017. Radioactive seepage through groundwater flow from the uranium minesNamibia. *Hydrology* 4 (1), 11. <https://doi.org/10.3390/hydrology4010011>
- Alarcón-Herrera, M.T., Bundschuh, J., Nath, B., Nicoll, H.B., Gutierrez, M., Reyes-Gomez, V.M., Nuñez, D., Martín-Dominguez, I.R., Sracek, O., 2013. Co-occurrence of arsenic and fluoride in groundwater of semi-arid regions in Latin America: genesis, mobility and remediation. *J. Hazard. Mater.* 262, 960–969.
- Alcaine, A.A., Schulz, C., Bundschuh, J., Jacks, G., Thunvik, R., Gustafsson, J., Mört, C.M., Sracek, O., Ahmad, A., Bhattacharya, P., 2020. Hydrogeochemical controls on the mobility of arsenic, fluoride and other geogenic co-contaminants in the shallow aquifers of northeastern La Pampa Province in Argentina. *Sci. Total Environ.* 715, 136671. <https://doi.org/10.1016/j.scitotenv.2020.136671>
- Alrakabi, M., Bhalla, A., Jatinder, G., Kumar, S., Singh, G., Mehta, D., Rai, B., Shahi, J.S., Singh, K.P., Singh, N., Srivathava, A., 2011. Uranium in groundwater water-logging in Malwa region. Scientific opinion & Fact sheet. Private Communication. Available: <http://www.indiaenvironmentportal.org.in/content/349547/uranium-in-ground-water-in-malwa-region-scientific-opinion-fact-sheet/>. (Accessed 8 March 2021).

- Bajwa, B.S., Kumar, S., Singh, S., Sahoo, S.K., Tripathi, R.M., 2017. Uranium and other heavy toxic elements distribution in the drinking water samples of SW-Punjab, India. *J. Radioanal Nucl. Chem.* 10, 13–19. <https://doi.org/10.1016/j.jrasc.2015.01.002>.
- Bangotra, P., Sharma, M., Mehra, R., Jakhu, R., Singh, A., Gautam, A.S., Gautam, S., 2021. A systematic study of uranium retention in human organs and quantification of radiological and chemical doses from uranium ingestion. *Environ. Technol. Innov.* 21, 101360. <https://doi.org/10.1016/j.eti.2021.101360>.
- Bhattacharya, P., Claesson, M., Bundschuh, J., Sracek, O., Fagerberg, J., Stomiolo, A.R., Thir, J.M., 2006. Distribution and mobility of arsenic in the rio Dulce alluvial aquifer in Santiago del Estero Province, Argentina. *Sci. Total Environ.* 358, 97–120.
- Bonotto, D.M., Wijesiri, B., Goonetilleke, A., 2019. Nitrate-dependent uranium mobilisation in groundwater. *Sci. Total Environ.* 693, 133655. <https://doi.org/10.1016/j.scitotenv.2019.133655>.
- Brunt et al., 2004 R. Brunt L. Vasak J. Griffioen 2004. Fluoride in groundwater: probability of occurrence of excessive concentration on global scale. International groundwater resources assessment centre report (IGRAC), Report nr. SP 2004–2012. IGRAC, Utrecht, p 9. <https://www.un-igrac.org/resource/fluoride-groundwater-probability-occurrence-excessive-concentration-global-scale> (Accessed 1 August 2021).
- Bundschuh, J., Farías, B., Martin, R., Stomiolo, A., Bhattacharya, P., Cortes, J., Bonorino, G., Albouy, R., 2004. Groundwater arsenic in the Chaco-Pampian Plain, Argentina: case study from Robles county, Santiago del Estero Province. *Appl. Geochem.* 19 231–14.
- Cao, B.W., Choo, C.O., 2019. Geochemical behavior of uranium and radon in groundwater of Jurassic Granite Area, Icheon, Middle Korea. *Water* 11, 1278. <https://doi.org/10.3390/w11061278>.
- Catalano, J.G., McKinley, J.P., Zachara, J.M., Smith, S.C., Brown, G.E., 2006. Changes in uranium speciation through a depth sequence of contaminated Hanford sediments. *Environ. Sci. Technol.* 40, 2517–2524. <https://doi.org/10.1021/es0520969>.
- Central Ground Water Board (CGWB) report, 2014. Water Quality Issues and Challenges in Punjab. <http://cgwb.gov.in/WQ/Punjab%20Book%20Final%20for%20Printing.pdf>. (Accessed 25 July 2021).
- Central Ground Water Board (CGWB) report, 2019. National Compilation on Dynamic Ground Water Resources of India, 2017. <http://cgwb.gov.in/GW-Assessment/GWRA-2017-National-Compilation.pdf>. (Accessed 25 July 2021).
- Central Ground Water Board (CGWB) report, 2020. Uranium occurrence in shallow aquifers in India. http://cgwb.gov.in/WQ/URANIUM_REPORT_2019-20.pdf. (Accessed 8 January 2021).
- Central Ground Water Board (CGWB) report, 2021. Ground Water Year Book Punjab And Chandigarh (UT), North Western Region Chandigarh. <http://cgwb.gov.in/Regions/NWR/Reports/Year%20Book%20Punjab%20and%20Chandigarh%20UT%202019-20.pdf>. (Accessed 20 July 2021).
- Chandrasekar, T., Sabarathinam, C., Viswanathan, P.M., Rajendiran, T., Mathivanan, M., Natesan, D., Samayamanthula, D.R., 2021. Potential interplay of uranium with geochemical variables and mineral saturation states in groundwater. *Appl Water Sci* 11, 1–18. <https://doi.org/10.1007/s13201-021-01396-3>.
- Cheng, T., Barnett, M.O., Roden, E.E., Zhuang, J., 2004. Effects of phosphate on uranium (VI) adsorption to goethite-coated sand. *Sci. Total Environ.* 38, 6059–6065. <https://doi.org/10.1021/es0403880>.
- Clark, D.L., Hobart, D.E., Neu, M.P., 1995. Actinide carbonte complexes and their importance in actinide environmental chemistry. *Chem. Rev.* 95 (1), 25–48. <https://doi.org/10.1021/cr00033a002>.
- Conceicao, F.T., Bonotto, D.M., 2000. Anthropogenic influences on the uranium concentration in waters of the Corumbatá river basin (SP), Brazil. *Revista Brasileira de Geociências* 30 (3), 555–557.
- Coyte, R.M., Jain, R.C., Srivastav, S.K., Sharma, K.C., Khalil, A., Ma, L., Vengosh, A., 2018. Large-scale uranium contamination of groundwater resources in India. *Environ. Sci. Technol. Lett.* 5, 341–347. <https://doi.org/10.1021/acs.estlett.8b00215>.
- Cumberland, S.A., Douglas, G., Grice, K., Moreau, J.W., 2016. Uranium mobility in organic matter-rich sediments: a review of geological and geochemical processes. *Earth Sci. Rev.* 159, 160–185. <https://doi.org/10.1016/j.earscirev.2016.05.010>.
- Das, N., Kumar, M., 2018. Co-occurrence of arsenic, fluoride and uranium in a fluvial environment EGU2018-Session HSS13 – Controls of Arsenic in Drinking water- Source water quality, compliance and implementation of drinking water safety plan at EGU General Assembly 2018, Vienna, Austria 8–13th April, 2018.
- Das, N., Sarma, K.P., Patel, A.K., Deka, J.P., Das, A., Kumar, A., Shea, P.J., Kumar, M., 2017. Seasonal disparity in the co-occurrence of arsenic and fluoride in the aquifers of the Brahmaputra flood plains, Northeast India. *Environ. Earth Sci.* 76, 183.
- Das, N., Das, A., Sarma, K.P., Kumar, M., 2018. Provenance, prevalence and health perspective of co-occurrences of arsenic, fluoride and uranium in the aquifers of the Brahmaputra River floodplain. *Chemosphere* 194, 755–772. <https://doi.org/10.1016/j.chemosphere.2017.12.021>.
- Del Nero, M., Galindo, C., Barillon, R., Madé, B., 2011. TRLFS evidence for precipitation of uranyl phosphate on the surface of alumina: environmental implications. *Environ. Sci. Technol.* 45, 3982–3988. <https://doi.org/10.1021/es2000479>.
- Department of Water Supply and Sanitation (DWSS), Ministry of Water Resources, Government of India. [Online]. Available: www.indiawater.gov.in/IMISReports. (Accessed 20 July 2021).
- Deutsch, W., 1997. Groundwater geochemistry: fundamentals and applications to contamination. Lewis Publishers, New York. <https://doi.org/10.1201/9781003069942>.
- Dong, W., Brooks, S.C., 2008. Formation of aqueous MgUO₂ (CO₃)₃₂ – complex and uranium anion exchange mechanism onto an exchange resin. *Environ. Sci. Technol.* 42 (6), 1979–1983. <https://doi.org/10.1021/es0711563>.
- Drage, J., Kennedy, G.W., 2013. Occurrence and Mobilization of Uranium in Groundwater in Nova Scotia. Geo Montreal. Nova Scotia Department of Natural Resources Mineral Resources Branch Contribution Series ME 2013-001. https://novascotia.ca/natr/meb/data/pubs/cs_me_2013-001.pdf. (Accessed 23 July 2021).
- Finch, R., Murakami, T., 1999. 2018. Systematics and paragenesis of uranium minerals. In: Burns, P.C., Finch, R. (Eds.), *Uranium: Mineralogy, Geochemistry and the Environment*. vol. 38. Mineralogical Society of America, Washington, DC, pp. 91–180. <https://doi.org/10.1515/9781501509193-008>.
- Freeze, R.A., Cherry, J.A., 1979. Groundwater. 604 pp Prentice-Hall, Englewood Cliffs, New Jersey. <https://www.un-igrac.org/sites/default/files/resources/files/Groundwater%20book%20-%20English.pdf>.
- Grybos, M., Davranche, M., Gruau, G., Petitjean, P., 2007. Is trace metal release in wetland soils controlled by organic matter mobility or Fe-oxyhydroxides reduction? *J. Colloid Interface Sci.* 314, 490–501. <https://doi.org/10.1016/j.jcis.2007.04.062>.
- GSI (Geological Survey of India), 2011. India water portal. <https://www.indiawaterportal.org/articles/state-geology-and-mineral-maps-geological-survey-india-miscellaneous-publication-series>. (Accessed 21 January 2021).
- Gupta, S., 2011. Central Ground Water Board, Ground Water Management in Alluvial Areas. . <http://cgwb.gov.in/documents/papers/incidpapers/paper%2011-%20sushil%20gupta.pdf>. (Accessed 27 July 2021).
- Guthrie, V.A., Kleeman, J.D., 1986. Changing uranium distributions during weathering of granite. *Chem. Geol.* 54, 113–126. [https://doi.org/10.1016/0009-2541\(86\)90075-6](https://doi.org/10.1016/0009-2541(86)90075-6).
- Hem, J.D., 1985. Study and interpretation of the chemical characteristics of natural waters. United States Geological Survey, Water Supply Paper 1473. USGS, Washington, D.C. <https://pubs.usgs.gov/wsp/wsp2254/pdf/wsp2254a.pdf>. (Accessed 30 July 2021).
- IARC (International Agency for Research on Cancer), 2013. Agents classified by the IARC monographs, volumes 1–108. <http://monographs.iarc.fr/ENG/Classification/index.php>. (Accessed 20 July 2021).
- Ijumulana, J., Ligate, F., Bhattacharya, P., Mtalo, F., Chaosheng, Z., 2020. Spatial analysis and GIS mapping of regional hotspots and potential health risk of fluoride concentrations in groundwater of northern Tanzania. *Sci. Total Environ.* 735, 139584. <https://doi.org/10.1016/j.scitotenv.2020.139584>.
- Jaswal, V., Kumar, R., Sahoo, P.K., Mittal, S., Kumar, A., Sahoo, S.K., Nandabalan, Y.K., 2021. Multi-parametric groundwater quality and human health risk assessment Vis-à-Vis hydrogeochemical process in an Agri-intensive region of Indus basin, Punjab, India. *Toxin Rev.* 1–17. <https://doi.org/10.1080/15569543.2021.1929324>.
- Jerden Jr., J.L., Sinha, A.K., 2003. Phosphate based immobilization of uranium in an oxidizing bedrock aquifer. *J. Appl. Geochem.* 18, 823–843. [https://doi.org/10.1016/S0883-2927\(02\)00179-8](https://doi.org/10.1016/S0883-2927(02)00179-8).
- Kaur, G., Kumar, R., Mittal, S., Sahoo, P.K., Vaid, U., 2021. Ground/drinking water contaminants and cancer incidence: a case study of rural areas of south West Punjab, India. *Hum. Ecol. Risk Assess.* 27, 205–226. <https://doi.org/10.1080/10807039.2019.1705145>.
- Keesari, T., Kulkarni, U.P., Deodhar, A., Ramanjaneyulu, P.S., Sanjukta, A.K., Kumar, U.S., 2014. Geochemical characterization of groundwater from an arid region in India. *Environ. Earth Sci.* 71, 4869–4888. <https://doi.org/10.1007/s12665-013-2878-x>.
- Krestou, A., Panias, D., 2004. Uranium (VI) speciation diagrams in the UO₂2+ / CO₃²⁻ / H₂O system at 25 °C. *European Journal of Mineral Processing & Environmental Protection* 4 (2), 113–129 1999.
- Krishnan, G., Kumar, B., Sudarsan, N., Rao, M.S., Ghosh, N.C., Taloor, A.K., Bhattacharya, P., Singh, S., Kumar, C.P., Sharma, A., Jain, S.K., Sidhu, B.S., Kumar, S., Vasisth, 2021. Isotopes (81O, 8D and 3H) variations in groundwater with emphasis on salinization in the state of Punjab, India. *Sci. Total Environ.* 789, 148051. <https://doi.org/10.1016/j.scitotenv.2021.148051>.
- Kumar, M., Kumari, K., Singh, U.K., Ramanathan, A.L., 2009. Hydrogeochemical processes in the groundwater environment of Muktsar, Punjab: conventional graphical and multivariate statistical approach. *Environ. Geol.* 57, 873–884.
- Kumar, A., Rout, S., Narayanan, U., Mishra, M.K., Tripathi, R.M., Singh, J., Kushwaha, H.S., 2011a. Geochemical modelling of uranium speciation in the subsurface aquatic environment of Punjab State in India. *J. Geol. Min. Res.* 3 (5), 137–146. <https://doi.org/10.5897/JGMR.9000028>.
- Kumar, A., Tripathy, R.M., Sabyasachi, R., Mishra, M.K., Ravi, P.M., Ghosh, A.K., 2014. Characterization of groundwater composition in Punjab state with special emphasis on uranium content, speciation and mobility. *Radiochim. Acta* 102, 239–254. <https://doi.org/10.1515/ract-2014-2109>.
- Kumar, M., Das, A., Das, N., Goswami, R., Singh, U.K., 2016. Co-occurrence perspective of arsenic and fluoride in the groundwater of Diphu, Assam, Northeastern, India. *Chemosphere* 150, 227–238.
- Kumar, M., Goswami, R., Patel, A.K., Srivastava, M., Das, N., 2020a. Scenario, perspectives and mechanism of arsenic and fluoride co-occurrence in the groundwater: a review. *Chemosphere* 249, 124126.
- Kumar, M., Kaushal, A., Sahoo, B.K., Sarin, A., Mehra, R., Jakhu, R., Sharma, N., 2019. Measurement of uranium and radon concentration in drinking water samples and assessment of ingestion dose to local population in Jalandhar district of Punjab, India. *Indoor Built Environ.* 28, 611–618. <https://doi.org/10.1177/1420326X17703773>.
- Kumar, R., Mittal, S., Peechat, S., Sahoo, P.K., Sahoo, S.K., 2020b. Quantification of groundwater-agricultural soil quality and associated health risks in the Agri-intensive Sutlej River basin of Punjab, India. *Environ. Geochem. Health* 42, 4245–4268. <https://doi.org/10.1007/s10653-020-00636-w>.
- Kumar, R., Mittal, S., Sahoo, P.K., Sahoo, S.K., 2021. Source apportionment, chemometric pattern recognition and health risk assessment of groundwater from southwestern Punjab, India. *Environ. Geochem. Health* 43, 733–755. <https://doi.org/10.1007/s10653-020-00518-1>.
- Kumar, A., Usha, N., Sawant, P.D., Tripathi, R.M., Raj, S.S., Mishra, M., Kushwaha, H.S., 2011b. Risk assessment for natural uranium in subsurface water of Punjab State, India. *Hum. Ecol. Risk Assess.* 17, 381–393. <https://doi.org/10.1080/10807039.2011.552395>.
- Langmuir, D., 1978. Uranium solution-mineral equilibria at low temperatures with applications to sedimentary ore deposits. *Geochim. Cosmochim. Acta* 42, 547–569. [https://doi.org/10.1016/0016-7037\(78\)90001-7](https://doi.org/10.1016/0016-7037(78)90001-7).
- Lapworth, D.J., Krishan, G., MacDonald, A.M., Rao, M.S., 2017. Groundwater quality in the alluvial aquifer system of northwest India: new evidence of the extend of anthropogenic

- and geogenic contamination. *Sci. Total Environ.* 599, 1433–1444. <https://doi.org/10.1016/j.scitotenv.2017.04.223>.
- Li, S., Wang, X., Huang, Z., Du, L., Tan, Z., Fu, Y., Wang, X., 2016. Sorption and desorption of uranium (VI) on GMZ bentonite: effect of pH, ionic strength, foreign ions and humic substances. *J. Radioanal. Nucl. Chem.* 308, 877–886. <https://doi.org/10.1007/s10967-015-4513-7>.
- Luo, W., Gao, X., Zhang, X., 2018. Geochemical processes controlling the groundwater chemistry and fluoride contamination in the Yuncheng Basin, China—an area with complex hydrogeochemical conditions. *PloS one* 13 (7), e0199082. <https://doi.org/10.1371/journal.pone.0199082>.
- Maher, K., Bargar, J.R., Brown Jr., G.E., 2013. Environmental speciation of actinides. *Inorg. Chem.* 52, 3510–3532. <https://doi.org/10.1021/ic301686d>.
- Makubalo, S.S., Diamond, R.E., 2020. Hydrochemical evolution of high uranium, fluoride and nitrate groundwaters of Namakwaland, South Africa. *J. Afr. Earth Sci.* 172 (104002), 1–32.
- Mehra, R., Singh, S., Singh, K., 2007. Uranium studies in water samples belonging to Malwa region of Punjab, using track etching technique. *Radiat. Meas.* 42, 441–445.
- Mittal, S., Sahoo, P.K., Sahoo, S.K., Kumar, R., Tiwari, R.P., 2021. Hydrochemical characteristics and human health risk assessment of groundwater in the Shivalik region of Sutlej basin, Punjab, India. *Arab. J. Geosci.* 14, 1–18. <https://doi.org/10.1007/s12517-021-07043-0>.
- Mukherjee, A., Scanlon, B.R., Fryar, A.E., Saha, D., Ghosh, A., Chaudhari, S., Mishra, R., 2012. Solute chemistry and fate of arsenic in the aquifers between the himalayan foothills and indian craton: influence of geology and geomorphology. *Geochim. Cosmochim. Acta* 90, 283–302. <https://doi.org/10.1016/j.gca.2012.05.015>.
- Mukherjee, A., Saha, D., Harvey, C.F., Taylor, R.G., Ahmed, K.M., Bhanja, S.N., 2015. Groundwater systems of the Indian sub-continent. *J. Hydrol. Reg. Stud.* 4, 1–14. <https://doi.org/10.1016/j.ejrh.2015.03.005>.
- Mukherjee, A., Scanlon, B., Aureli, A., Langan, S., Guo, H., McKenzie, A., 2020. *Global Groundwater: Source, Scarcity, Sustainability, Security and Solutions*. first ed. Elsevier 9780128181720.
- Nasher, N.M.R., Ahmed, Md.H., 2021. Groundwater geochemistry and hydrogeochemical processes in the Lower Ganges-Brahmaputra-Meghna River Basin areas, Bangladesh. *J. Asian Earth Sci.* 6, 100062.
- O'Loughlin, E.J., Boyanov, M.I., Antonopoulos, D.A., Kemner, K.M., 2011. Redox processes affecting the speciation of technetium, uranium, neptunium, and plutonium in aquatic and terrestrial environments. In: Tratnyek, P.G., Grundl, T.J., Haderlein, S.B. (Eds.), *Aquatic Redox Chemistry*, ACS Symposium Series. vol. 1071. American Chemical Society, pp. 477–517. <https://doi.org/10.1021/bk-2011-1071.ch022>.
- Pant, D., Keesari, T., Sharma, D., Rishi, M., Singh, G., Jaryal, A., Tripathi, R.M., 2017. Study on uranium contamination in groundwater of Faridkot and Muktsar districts of Punjab using stable isotopes of water. *J. Radioanal. Nucl. Chem.* 313, 635–639. <https://doi.org/10.1007/s12665-020-8818-7>.
- Patel, A.K., Das, N., Goswami, R., Kumar, M., 2019a. Arsenic mobility and potential co-leaching of fluoride from the sediments of three tributaries of the Upper Brahmaputra floodplain, Lakhimpur, Assam, India. *J. Geochem. Explor.* 203, 45–58.
- Patel, A.K., Das, N., Kumar, M., 2019b. Multilayer arsenic mobilization and multimetal co-enrichment in the alluvium (Brahmaputra) plains of India: a tale of redox domination along the depth. *Chemosphere* 224, 140–150.
- Patnaik, R., Lahiri, S., Chahar, V., Naskar, N., Sharma, P.K., Avhad, D.K., Bassan, M.K.T., Knolle, F., Schnug, E., Srivastava, A., 2016. Study of uranium mobilization from Himalayan Siwaliks to the Malwa region of Punjab state in India. *J. Radioanal. Nucl. Chem.* 308, 913–918. <https://doi.org/10.1007/s10967-015-4578-3>.
- Payne, T.E., Davis, J.A., Waite, T.D., 1996. Uranium adsorption on ferrihydrite—effects of phosphate and humic acid. *Radiochim. Acta* 74, 239–243. <https://doi.org/10.1524/ract.1996.74.special-issue.239>.
- Piper, A.M., 1944. A graphic procedure in the geochemical interpretation of water analyses. *Am. Geophys. Union Trans.* 25, 914–923.
- Purushothaman, P., Rao, M.S., Rawat, Y.S., Kumar, C.P., Krishan, G., Parveen, T., 2014. Evaluation of hydrogeochemistry and water quality in Bist-Doab region, Punjab, India. *Environ. Earth Sci.* 72, 693–706. <https://doi.org/10.1007/s12665013-2992-9>.
- Rajmohan, N., Elango, L., 2003. Identification and evolution of hydrogeochemical processes in the groundwater environment in an area of the Palar and Cheyyar River Basins, Southern India. *Environ. Geol.* <https://doi.org/10.1007/s00254-004-1012-5>.
- Rashid, A., Guan, D.X., Farooqi, A., Khan, S., Zahir, S., Jehan, S., Khattak, S.A., Khan, M.S., Khan, R., 2018. Fluoride prevalence in groundwater around a fluorite mining area in the flood plain of the river swat, Pakistan. *Sci. Total Environ.* 635, 203–215. <https://doi.org/10.1016/j.scitotenv.2018.04.064>.
- Riedel, T., Kubick, C., 2018. Uranium in groundwater – a synopsis based on a large hydrogeochemical data set. *Water Res.* 129, 29–38. <https://doi.org/10.1016/j.watres.2017.11.001>.
- Rishi, M.S., Keesari, T., Sharma, D.A., Pant, D., Sinha, U.K., 2017. Spatial trends in uranium distribution in groundwaters of Southwest Punjab, India—a hydrochemical perspective. *J. Radioanal. Nucl. Chem.* 311, 1937–1945. <https://doi.org/10.1007/s10967-017-5178-1>.
- Ritz, R.W., Wright, S.L., Mann, B., Chen, M., 1993. Analysis of temporal variability in hydrogeochemical data used for multivariate analyses. *Groundwater* 31, 221–229.
- Rout, S., Ravi, P.M., Kumar, A., Tripathy, R.M., 2015. Study on speciation and salinity-induced mobility of uranium from soil. *Environ. Earth Sci.* 74, 2273–2281. <https://doi.org/10.1007/s12665-015-4218-9>.
- Roy, P.S., Meiyappan, P., Joshi, P.K., Kale, M.P., Srivastava, V.K., Srivastava, S.K., Behera, M.D., Roy, A., Sharma, Y., Ramachandran, R.M., Bhavani, P., Jain, A.K., Krishnamurthy, Y.V.N., 2016. Decadal Land Use and Land Cover Classifications across India, 1985, 1995, 2005. ORNL DAAC, Oak Ridge, Tennessee, USA. <https://doi.org/10.3334/ORNLDAAC/1336>.
- Rump, A., Eder, S., Lamkowski, C., Hermann, C., Abend, M., Port, M., 2019. A quantitative comparison of the chemo- and radiotoxicity of uranium at different enrichment grades. *Toxicol. Lett.* 323, 159–168. <https://doi.org/10.1016/j.toxlet.2019.07.004>.
- Salama, R.B., Otto, C.J., Fitzpatrick, R.W., 1999. Contributions of groundwater conditions to soil and water salinization. *Hydrogeol. J.* 7, 46–64. <http://link.springer.de/link/service/journals/10040>.
- Scanlon, B.R., Nicot, J.P., Reedy, R.C., Kurtzman, D., Mukherjee, A., Nordstrom, D.K., 2009. Elevated naturally occurring arsenic in a semiarid oxidizing system, Southern High Plains aquifer, Texas, USA. *Appl. Geochem.* 24, 2061–2071.
- Schoeller, H., 1967. *Geochemistry of groundwater. An international guide for research and practice*. 15. UNESCO, pp. 1–18 Chap.
- Seder-Colomina, M., Morin, G., Brest, J., Ona-Nguema, G., Gordien, N., Pernelle, J.J., van Hullebusch, E.D., 2015. Uranium (VI) scavenging by amorphous iron phosphate encrusting Sphaerotilus natans Filaments. *Environ. Sci. Technol.* 49, 14065–14075. <https://doi.org/10.1021/acs.est.5b03148>.
- Seder-Colomina, M., Morin, G., Brest, J., Ona-Nguema, G., Gordien, N., Pernelle, J.J., van Hullebusch, E.D., 2015. Uranium (VI) scavenging by amorphous iron phosphate encrusting Sphaerotilus natans Filaments. *Environ. Sci. Technol.* 49, 14065–14075. <https://doi.org/10.1021/acs.est.5b03148>.
- Sharma, A.D., Rishi, M.S., 2016. Presence of uranium in groundwater of Punjab: an overview. In: Raju, N. (Ed.), *Geostatistical and Geospatial Approaches for the Characterization of Natural Resources in the Environment*. Springer, Cham, pp. 231–236. https://doi.org/10.1007/978-3-319-18663-4_36.
- Sharma, N., Singh, J., 2016. Radiological and chemical risk assessment due to high uranium contents observed in the ground waters of Mansa District (Malwa region) of Punjab state, India: an area of high cancer incidence. *Expo Health* 8, 513–525. <https://doi.org/10.1007/s12403-016-0215-9>.
- Sharma, N., Singh, J., 2017. Human kidney and skeleton uranium burden, radiation dose and health risks from high uranium contents in drinking water of Bathinda district (Malwa region) of Punjab state, India. *Radiat. Prot. Dosim.* 176, 242–251. <https://doi.org/10.1093/rpd/ncx002>.
- Sharma, T., Sharma, A., Kaur, I., Mahajan, R.K., Litoria, P.K., Sahoo, S.K., Bajwa, B.S., 2019. Uranium distribution in groundwater and assessment of age dependent radiation dose in Amritsar, Gurdaspur and Pathankot districts of Punjab, India. *Chemosphere* 219, 607–616. <https://doi.org/10.1016/j.chemosphere.2018.12.039>.
- Sharma, T., Bajwa, B.S., Kaur, I., 2021. Contamination of groundwater by potentially toxic elements in groundwater and potential risk to groundwater users in the Bathinda and Faridkot districts of Punjab, India. *Environ. Earth Sci.* 80, 1–15. <https://doi.org/10.1007/s12665-021-09560-3>.
- Sharma, T., Litoria, P.K., Bajwa, B.S., Kaur, I., 2021. Appraisal of groundwater quality and associated risks in Mansa district (Punjab, India). *Environ. Monit. Assess.* 193, 1–21. <https://doi.org/10.1007/s10661-021-08892-8>.
- Singh, J., Singh, L., Singh, S., 1995. High U-contents observed in some drinking waters of Punjab, India. *Journal of Environmental Radioactivity* 26 (3), 217–222. [https://doi.org/10.1016/0265-931X\(94\)00037-W](https://doi.org/10.1016/0265-931X(94)00037-W).
- Singh, L., Kumar, R., Kumar, S., Bajwa, B., Singh, S., 2013. Health risk assessments due to uranium contamination of drinking water in Bathinda region, Punjab state, India. *Radioprotection* 48, 191–202. <https://doi.org/10.1051/RADIOPRO/2012042>.
- Singh, K.P., Kishore, N., Tuli, N., Loyal, R.S., Kaur, M., Taak, J.K., 2018. Uranium contamination of groundwater in Southwest Parts of Punjab State, India, with special reference to role of basement granite. In: Saha, D., Marwaha, S., Mukherjee, A. (Eds.), *Clean and Sustainable Groundwater in India. Springer Hydrogeology*. Springer, Singapore https://doi.org/10.1007/978-981-10-4552-3_7.
- Smedley, P.L., Nicoll, H.B., Macdonald, D.M.J., Barros, A.J., Tullio, J.O., 2002. Hydrogeochemistry of arsenic and other inorganic constituents in groundwaters from La Pampa Argentina. *Appl. Geochem.* 17, 259–284.
- Smedley, P., Smith, B., Abesser, C., D. L., 2006. Uranium occurrence and behaviour in British groundwater. *British Geological Survey* 1050 2006 [Report No.: CR/06/050 N].
- Stewart, B.D., Amos, R.T., Nico, P.S., Fendorf, S., 2011. Influence of uranyl speciation and iron oxides on uranium biogeochemical redox reactions. *Geomicrobiol. J.* 28, 444–456. <https://doi.org/10.1080/01490451.2010.507646>.
- Sturchio, N.C., Banner, J.L., Binz, C.M., Heraty, L.B., Musgrove, M., 2001. Radium geochemistry of ground waters in paleozoic carbonate aquifers, midcontinent, USA. *App. Geochem.* 16, 109–122. [https://doi.org/10.1016/S0883-2927\(00\)0014-7](https://doi.org/10.1016/S0883-2927(00)0014-7).
- Thivya, C., Chidambaram, S., Keesari, T., Prasanna, M.V., Thilagavathi, R., Adithya, V.S., Singaraja, C., 2016. Lithological and hydrochemical controls on distribution and speciation of uranium in groundwaters of hard-rock granitic aquifers of Madurai District, Tamil Nadu (India). *Environ. Geochem. Health* 38, 497–509. <https://doi.org/10.1007/s10653-015-9735-7>.
- USEPA, 1989. Risk assessment guidance for superfund, Vol I, Human health evaluation manual (Part A). Office of Emergency and Remedial Response, Washington, DC. https://www.epa.gov/sites/default/files/2015-09/documents/rags_a.pdf. (Accessed 15 July 2021).
- USEPA, 2001. Diazinon revised risk assessment and agreement with registrants. Fact sheet, available at <http://www.epa.gov/opprrd1/op/diazinon/agreementjan.pdf> (Accessed 15 July 2021).
- Veeramani, H., Scheinost, A.C., Monsegue, N., Qafoku, N.P., Kukkadapu, R., Newville, M., Lanzirotti, A., Pruden, A., Murayama, M., Hochella Jr., M.F., 2013. Abiotic reductive immobilization of U (VI) by biogenic mackinawite. *Environ. Sci. Technol.* 47, 2361–2369. <https://doi.org/10.1021/es304025x>.
- Virk, H.S., 2016. Measurement of concentration of natural uranium in ground waters of bathinda district (S. Punjab) for the assessment of annual effective dose. *Env Sci & Disaster Management* 16, 25–29 ISSN: 2249-460x & Print ISSN: 0975-587X.
- Virk, H.S., 2017a. Uranium content anomalies in groundwaters of Ferozepur District of Punjab (India) and the corresponding risk factors. *Research & Reviews: J Oncol Hematol.* 6 (3) 18–24p. ISSN: 2319-3387 (Online).
- Virk, H.S., 2017b. Uranium content anomalies in groundwaters of Fazilka District of Punjab (India) for the assessment of excess cancer risk. *Research & Reviews: J Oncol Hematol.* 6 (2), 21–26p. <https://doi.org/10.37591/rrjoh.v6i2.1475>.

- Virk, H.S., 2019a. Uranium content anomalies in groundwater of Barnala District of Malwa Belt of Punjab (India) for the assessment of excess cancer risk. *Researc & Reviews: J Oncol Hematol.* 8. <https://doi.org/10.37591/rjrooh.v8i1.718> 19–26.
- WHO, 2017. *Guidelines for Drinking-Water Quality*. World Health Organization, Geneva.
- Wu, Y., Wang, Y., Xie, X., 2014. Occurrence, behavior and distribution of high levels of uranium in shallow groundwater at Datong basin, northern China. *Sci. Total Environ.* 472, 809–817. <https://doi.org/10.1016/j.scitotenv.2013.11.109>.
- Virk, H.S., 2019b. Uranium content anomalies in groundwater of Patiala District of Punjab (India) for the assessment of excess cancer risk. *Res.Rev.J. Oncol. Hematol.* 8 (2). <https://doi.org/10.37591/rjrooh.v8i2.1560> 13–19.
- Wu, Y., Li, J., Wang, Y., Xie, X., 2018. Variations of uranium concentrations in a multi-aquifer system under the impact of surface water-groundwater interaction. *J. Contam. Hydrol.* 211, 65–76. <https://doi.org/10.1016/j.jconhyd.2018.03.007>.
- Xiong, L., Alshamsi, D., Yi, P., Hou, X., Murad, A., Hussein, S., Aldahan, A., Mohamed, M., 2020. Distribution of uranium isotopes in groundwater of the UAE: envieonmental radioactivity assessment. *J. Radioanal. Nucl. Chem.* 325, 57–66. <https://doi.org/10.1007/s10967-020-07216-3>.
- Zamora, M.L., Tracy, B.L., Zielinski, J.M., Meyerhof, D.P., Moss, M.A., 1998. Chronic ingestion of uranium in drinking water: a study of kidney bioeffects in humans. *Toxicol. Sci.* 43, 68–77.